

MODELLING ACTIVATED CARBON ADSORPTION KINETICS FOR REMOVAL OF MICROPOLLUTANTS FROM WASTEWATER

Mathieu Coghe

Student number: 02207820

Promotors: Dr. Ir. Saba Daneshgar, Dr. Ir. Giacomo Bellandi

Tutors: Ir. Daniel Illana González, Ir. Simon Duchi

Master's Dissertation submitted to Ghent University in partial fulfilment of the requirements for the degree of
Master of Science in Environmental Science and Technology

Academic year: 2023 - 2024

Copyright

The author and the promoter give the permission to use this master dissertation for consultation and to copy parts of it for personal use. Every other use is subject to the copyright laws, more specifically the source must be extensively stated when using from this thesis.

De auteur en de promotor geven de toelating deze masterproef voor consultatie beschikbaar te stellen en delen van de masterproef te kopiëren voor persoonlijk gebruik. Elk ander gebruik valt onder de beperkingen van het auteursrecht, in het bijzonder met betrekking tot de verplichting de bron uitdrukkelijk te vermelden bij het aanhalen van resultaten uit deze masterproef.

Gent, 1 May 2024

The promoter(s),

The author,

'Signature'

Prof. + Name

'Signature'

'Name'

PREFACE

TABLE OF CONTENTS

| | |
|--|-----------|
| LIST OF ABBREVIATIONS | 6 |
| ABSTRACT | 7 |
| INTRODUCTION | 8 |
| 1.1 Problem statement: organic micropollutants | 8 |
| 1.2 Modelling removal of organic micropollutants | 9 |
| 1.3 Aim of the thesis | 9 |
| LITERATURE REVIEW | 11 |
| 1 Principles of micropollutant removal | 11 |
| 1.1 Classification of MPs | 11 |
| 1.2 The fate of micropollutants in WWTPs | 12 |
| 1.3 Tertiary treatment methods for MP removal in WWTPs | 14 |
| 1.4 The adsorption process | 19 |
| 1.5 Types of adsorbents | 20 |
| 1.6 Types of adsorption set-ups | 23 |
| 1.7 Adsorption equilibrium | 24 |
| 1.8 Adsorption kinetics | 25 |
| 1.9 The breakthrough curve | 26 |
| 2 Adsorption on activated carbon: Breakthrough curve models | 28 |
| 2.1 Opportunities and challenges | 28 |
| 2.2 Components of fixed-bed BTC models | 29 |
| 2.3 Equilibrium relationship: isotherm equations | 29 |
| 2.4 Fixed-bed BTC models | 32 |
| 2.5 Conclusion BTC models | 40 |
| MATERIALS AND METHODS | 42 |
| 3 USEPA PSDM model | 42 |
| 4 Article Modelling PFAS Removal using GAC | 44 |
| 5 Europe Interreg project and Aquafin | 47 |
| RESULTS AND DISCUSSION | 48 |
| 6 Testing the PSDM by USEPA model | 48 |
| 6.1 Isotherm fitting tool | 48 |

| | | |
|-----------------------|--|-----------|
| 6.2 | Example modelling of compound TCE | 49 |
| 6.3 | Pilot modelling of compound PFHpA | 50 |
| 6.4 | USEPA fouling approach | 51 |
| 7 | Extending the PSDM by USEPA model | 54 |
| 7.1 | Extending the USEPA fouling approach | 54 |
| 7.2 | Alternative fouling approach | 55 |
| 7.3 | Uncertainty analysis of Freundlich parameters | 57 |
| 8 | The PSDM model for full-scale application | 59 |
| 8.1 | The Interreg project | 59 |
| CONCLUSION | | 60 |
| REFERENCE LIST | | 61 |
| APPENDICES | | 69 |

LIST OF ABBREVIATIONS

Calibration =

Validation =

ABSTRACT

INTRODUCTION

As the Planetary Boundary for novel entities is now exceeding, it is priority to keep an eye on micropollutants in our aquatic effluents (Persson et al., 2022). Although they are invisible, organic micropollutants (OMPs) are among the most important environmental problems in the last decades (Mohammadi et al., 2022). Moreover, with increasing pharmaceutical and cosmetical care, the release of organic micropollutants into water bodies is expected to increase in the future. The European Union (EU) is enforcing more strict regulations on the discharge of these small but complex contaminants (Khanzada et al., 2020). There is more awareness of the importance of treatment concerning the high exposure and hazard of these OMPs.

1.1 Problem statement: organic micropollutants

The definition of organic micropollutants can be explained by putting the words apart: ‘organic’ substances that commonly occur in the environment in small concentrations (lower than 1 µg/L, ‘micro’) but are still considered ‘pollutants’ due to their biologically adverse effects at these trace concentrations (Spindola Vilela et al., 2022).

It is not surprising that micropollutants (MPs) are mainly of anthropogenic origin. They form a big group of pollutants, originating from a wide range of sources. Today, one counts more than 100 000 MPs that have been used by humans and animals for health care and lifestyle improvement. Typical organic micropollutants coming from industrial sources are perfluorinated compounds (per- and polyfluoroalkyl substances or PFAS), phenolic compounds and dyes. OMPs originating from agriculture are mainly pesticides. From pharmaceutical industry, pharmaceutical compounds are of big concern. Households are another source of micropollutants as pharmaceutics, compounds from personal care products and cleaning products end up in municipal wastewaters (Topolovec et al., 2022).

Next to health damage, Contaminants of Emerging Concern (CEC) are concerning because of damage to the environment through persistency, biomagnification and harmful algal blooms (HABs). Because these micropollutants are very small, tracking and risk assessment may be very difficult.

In the last decades, there is more awareness that MPs are present in our industrial and household effluents. Even after treatment by wastewater treatment plants (WWTPs), concentrations are still too high. They are only partially able to remove these pollutants because most of them are refractory to biological treatments and very persistent. This gives them the chance to accumulate in the environment and eventually in the food-chain (Guilossou et al., 2020; Pocostales et al., 2010). Typical sources and pathways of MPs are shown in **Figure 1**. The lack of treatment in conventional activated sludge (CAS) systems of these present and hazardous OMPs covers the problem statement in this script.

It is clear that advanced treatment is needed to prevent this pollution from escalating further. Several types of advanced treatment technologies are proposed in literature. Most of them are not ready for application on large scale because of their high operational costs, high installation costs, or lack of knowledge on how to use them properly. The use of granular activated carbon (GAC) for the removal of OMPs has been discussed in numerous papers. This mature adsorption technique has widely been applied for drinking water treatment. Further, the system is easily implemented in existing WWTPs: it can be used as post-process, also called tertiary process, after the conventional treatment processes (Aliakbarian et al., 2015; Ma et al., 2021; Šerban et al., 2023).

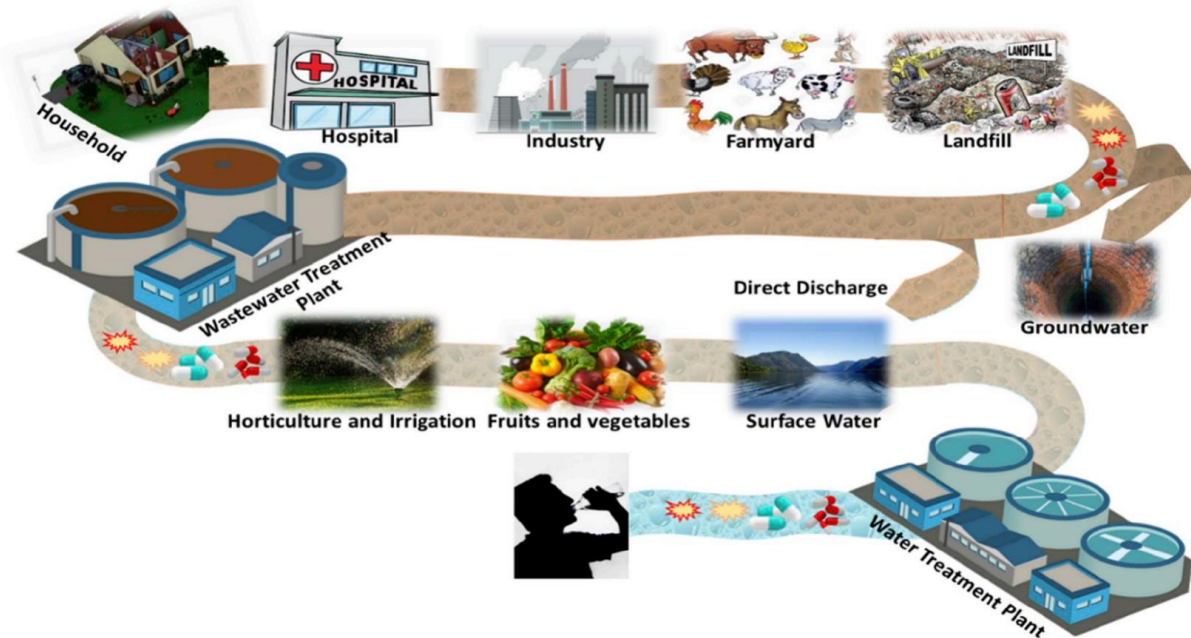


Figure 1 Sources and pathways of harmful micropollutants (Khanzada et al., 2020)

1.2 Modelling removal of organic micropollutants

A way to help find optimal solutions for removal of organic micropollutants, is modelling. As the first full-scale set-ups for OMPs treatment are rising, it is important to advice constructors with optimal performance conditions. These can be found by conducting pilot tests, but they are expensive and only a limited amount of conditions can be tested. Modelling can extend the amount of scenarios studied and assist dealing with current challenges of upscaling newly purposed technologies. This way, faster decision-making is possible so one can deal with more strict thresholds in the future. As more efforts are done to measure these very small concentrations, models can be validated with experimental data.

1.3 Aim of the thesis

The aim of the thesis is to investigate existing models for the removal of organic micropollutants through activated carbon adsorption, and to conduct a comparison, reliability and potential analysis. To do so, the following steps are undertaken:

- **Sketch the source and fate of micropollutants in wastewater treatment plants**
- **Address possible options for removal of organic micropollutants**
- **Study the adsorption process and its variability**
- **Explore and compare adsorption models**

One open-source model valuable for simulation of GAC adsorption is tested in Python. Its working mechanisms are studied and small extensions are made where useful. The current applicability of the model for full-scale prediction is analysed. Aquafin's set-up in Aartselaar is used as an example for full-scale application of municipal wastewater treatment (Aquafin, 2023). There, the traditional wastewater treatment plant is extended by tertiary treatment with a combination of ozonation ('Ozone contact tank') and activated carbon adsorption ('GAC filters'). These two tertiary treatment technologies and traditional treatment are illustrated in **Figure 2**. Parameters and concentrations are estimated from this set-up.

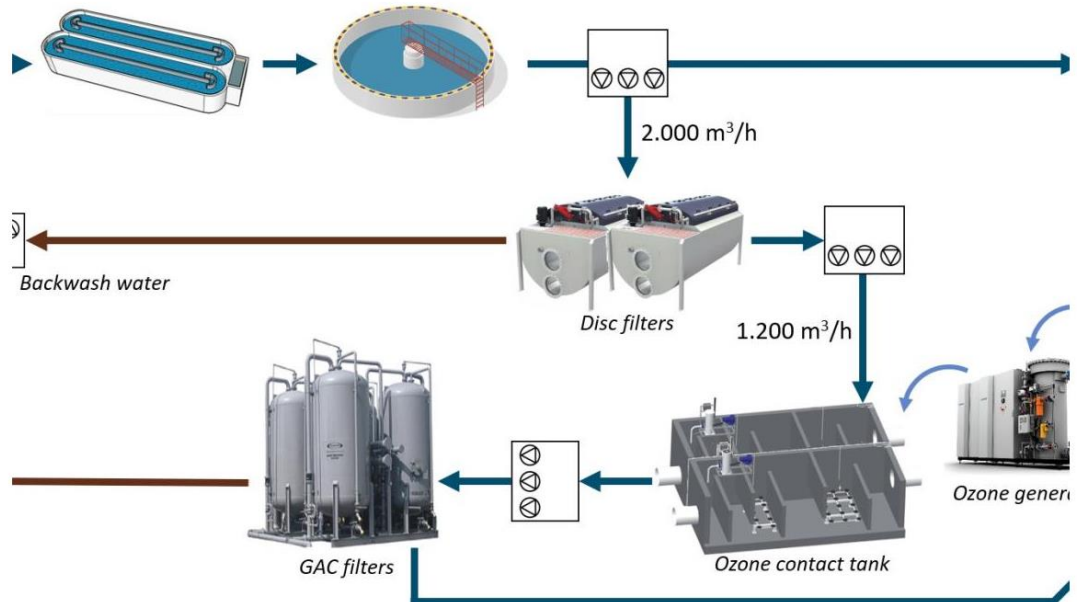


Figure 2 WWTP in Aartselaar with tertiary treatment extension, Ozone + GAC, for removal of micropollutants at full-scale (Aquafin, 2023)

LITERATURE REVIEW

1 PRINCIPLES OF MICROPOLLUTANT REMOVAL

1.1 Classification of MPs

Classification is mostly based on the source/sector or type of micropollutant. Regarding source, classes include pharmaceutical active compounds (PhACs), household personal care products (PCPs), agricultural pesticides and industrial chemicals (Khanzada et al., 2020).

Prevalent groups of OMPs within the PhACs class are antibiotics and hormones, which find their origin in hospitals. Adverse effects of antibiotics involve bacterial resistance. An example of hormones is estrogens and its adverse effects include endocrine disruption, which is why they are labelled as endocrine disrupting compounds (EDCs). Important groups of OMPs within the PCPs class are disinfectants, preservatives, insect repellents and sunscreen. Plastics and heavy metals are primarily inorganic micropollutants within the industrial chemicals class. Per- and polyfluoroalkyl substances (PFAS) are organic micropollutants within the industrial chemicals class and have still an important and essential function in fire retardants. Further on this class, phenolic compounds are worth mentioning as they are widely used in several industries thanks to their antioxidant, antimicrobial and anti-inflammatory properties, but are also classified as EDCs (Albuquerque et al., 2020). Finally, pesticides and herbicides are OMPs originating from the agricultural field and mostly disposed directly into water bodies.

Detailed classification in groups and subgroups of MPs, together with examples and adverse effects, can be found in (Das et al., 2017; Spindola Vilela et al., 2022). Organic micropollutants are not being listed in this report, but a brief, summarizing overview is shown in **Figure 3**. It can be seen that the three main sources of pollution by OMPs through WWTPs are households, hospitals and industries (European Investment Bank & Bofill, 2023).

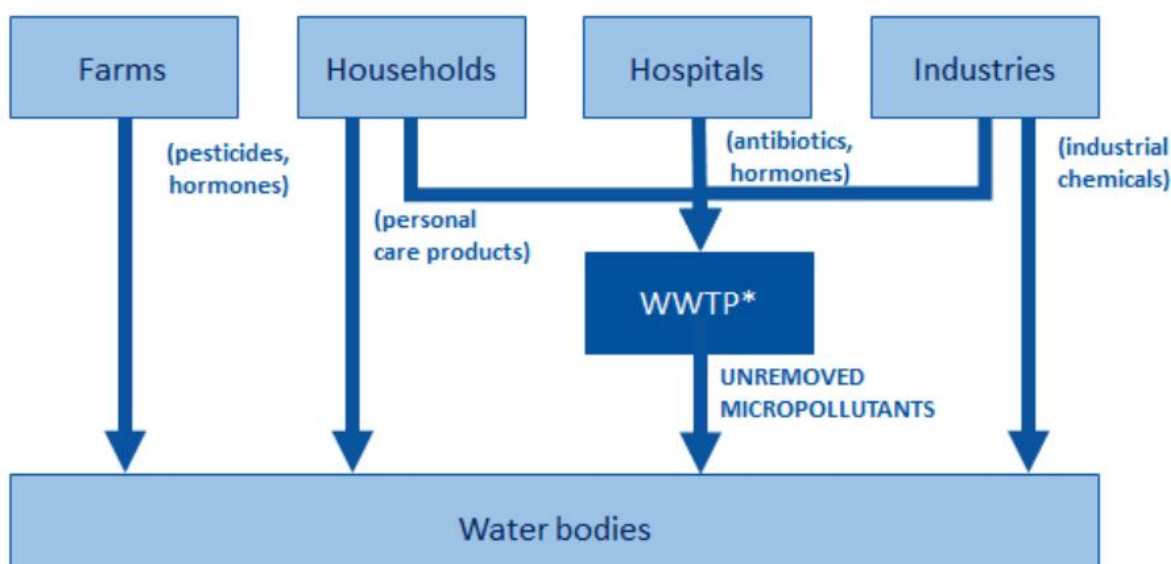


Figure 3 Classification by source and pathways of organic micropollutants, *wastewater treatment plant
(European Investment Bank & Bofill, 2023)

1.2 The fate of micropollutants in WWTPs

In typical wastewater treatment plants nowadays, there is partial removal of organic and inorganic micropollutants, through different pathways. An overview of all the relevant removal pathways in a WWTP is illustrated in **Figure 4**.

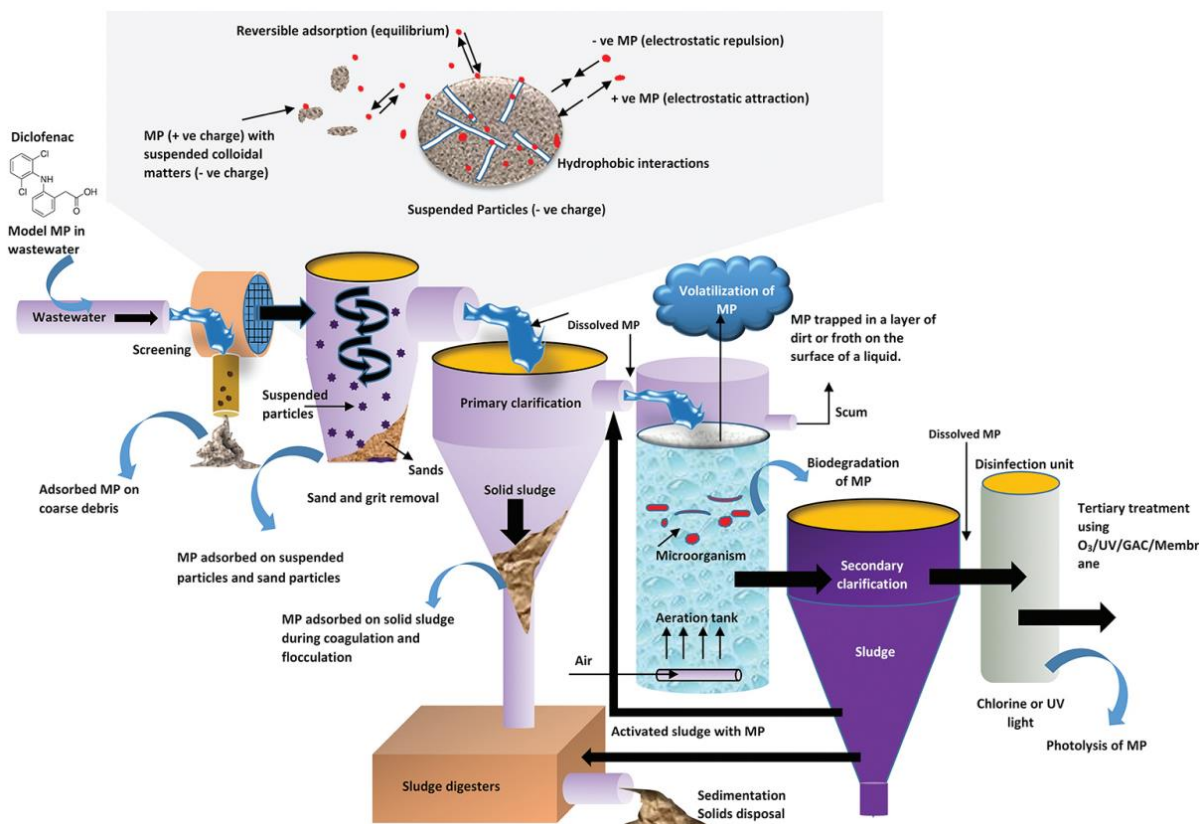


Figure 4 Fate and removal processes of micropollutants in a WWTP (Das et al., 2017)

Adsorption onto sediment in the primary treatment or biodegradation during the secondary treatment are the main removal fates of micropollutants in conventional activated sludge (CAS) systems. Some volatile MPs have potential to be removed by volatilization. However, conventional treatment in typical WWTPs is not sufficient in the removal of organic micropollutants. As stated in the introduction, treated effluent concentrations are still of concern. This is quantified in **Table 1**, where examples of CEC are listed per class with their respective removal efficiencies in CAS plants. It is clear that reported removal efficiencies are highly variable.

Some antibiotics such as Enrofloxacin do not feel any effect by the conventional treatment, while others, like sulfamethoxazole, decline in concentration. Estrogens like Enrofloxacin and Estrone (E1) have low up to high removal efficiency. The personal care product (PCP) in this table has limited removal (up to 55%). Industrial chemical compounds are again highly varying. What is remarkable is that some PFAS compounds can have negative removal efficiencies. The reference article has a declaration for this rising effluent concentration in their WWTP measurements. It declares that the enrichment of some PFAS may be caused by additional production via precursor degradation (Kim et al., 2012). Higher rates of formation are identified at higher HRT and temperature, due to the enhanced biological reactions (Guerra et al., 2014). Pesticides are mostly not reported in CAS systems because these compounds are of agricultural rather than urban origin (Krzeminski et al., 2019).

Table 1 Reported CEC removal efficiencies in CAS plants (Krzeminski et al., 2019)

| Class | CEC | Removal efficiency (%) |
|--|---------------------------------------|-----------------------------|
| Pharmaceutical active compounds (PhACs) | Sulfamethoxazole (antibiotics) | 35-84 |
| | Enrofloxacin (antibiotics) | ~0 |
| | Azithromycin (antibiotics) | 11-44 |
| | Estrone (estrogens) | 58-81 |
| | 17 α -Ethynodiol (estrogens) | 18-94 |
| Household personal care products (PCPs) | 2-Ethylhexyl ethoxycinnamate | 30-55 |
| Industrial chemicals | Butylated hydroxytoluene (phenolics) | 89 |
| | Tetrabromobisphenol A (phenolics) | 10-100 |
| | Hexabromocyclododecane | 0-86 |
| | Benzotriazole | 30-91 |
| | Perfluorobutanoic acid, PFBA (PFAS) | (-108)-65 |
| | Perfluoropentanoic acid, PFPeA (PFAS) | (-400)-50 |
| | Perfluorohexanoic acid, PFHxA (PFAS) | (-226)-39 |
| | Perfluoroheptanoic acid, PFHpA (PFAS) | (-32) (Guerra et al., 2014) |
| Agricultural pesticides | Methiocarb | N.A. |
| | Oxadiazon | N.A. |
| | Triallate | N.A. |

Traditional treatment by CAS plants are clearly not ideal for removal of CEC. Effluent concentrations are highly variable and in some cases even higher than the influent. The diversity of the chemical structure of course contributes to the high variance. Also, CEC removal efficiency is strongly affected by HRT and SRT (Krzeminski et al., 2019). The extreme variability makes it difficult to meet thresholds.

For this reason, additional treatment is required. This additional treatment, also called ‘advanced treatment’, is illustrated in **Figure 4** under the name ‘Tertiary treatment’. ‘O₃’ means that ozone is used through the ozonation process, a process where oxidation is applied to partially destroy micropollutants. With oxidation as method for MPs removal, ozonation belongs to the group of advanced oxidation processes (AOP). Another type of AOPs is ‘UV’, in which UV-light is used to produce oxidizing agents for degradation of the pollutants (Kumari & Kumar, 2023). ‘GAC’ and ‘Membrane’ are other types of tertiary treatment. With the growth of industry and emerging pollutants in the last decades, tertiary treatment is now essential before discharging the effluent in the environment and especially when water is reused for drinking purposes. Single and combined technologies are discussed in the next paragraph.

1.3 Tertiary treatment methods for MP removal in WWTPs

1.3.1 Single technologies for tertiary treatment

This paragraph provides an overview of advanced treatment processes currently available or have potential to remove micropollutants in wastewater treatment plants. A quantified approach based on removal efficiencies is not implemented in this study. This would be too summarized as it is limited to only certain MPs and certain conditions. Moreover, efficiency is not the only criteria for a good treatment technology. Here, a descriptive approach is adopted for the technology assessment. The most important treatment groups, their technologies, advantages and disadvantages, are listed in **Table 2**.

Table 2 Advantages and disadvantages of different methods for OMPs removal from wastewater

| Treatment group (TG) | Advantages TG | Disadvantages TG | Reference |
|--------------------------------------|--|--|---|
| Advanced oxidation process | Organic destruction | Residual by-products | (V. Sharma & Feng, 2017; Zahmatkesh, Amesho, et al., 2022) |
| - <i>UV-radiation</i> | Rapid reaction | Energy-intensive | |
| - <i>(Photo-)Fenton</i> | Disinfection | | |
| - <i>Sonolysis</i> | | | |
| - <i>Wet Air Oxidation</i> | | | |
| - <i>Ozonation</i> | | | |
| Membrane treatment | FO, MD low operating costs | High (re-)investment costs | (Khanzada et al., 2020; Rizzo et al., 2019; Zahmatkesh, Amesho, et al., 2022) |
| - <i>Reverse osmosis (RO)</i> | High efficiency | RO, NF energy intensive | |
| - <i>Nanofiltration (NF)</i> | Ions removal | Fouling and scaling | |
| - <i>Forward osmosis (FO)</i> | Disinfection | Concentrate | |
| - <i>Membrane distillation (MD)</i> | | | |
| Biological treatment | MPs degraded, transformed, mineralized (or absorbed) | High retention time Sludge generation | (Gutiérrez et al., 2021; Zahmatkesh, Amesho, et al., 2022) |
| Coagulation and flocculation* | Simple application | Transfer toxic compounds to solid phase | (Das et al., 2017; Zahmatkesh, Amesho, et al., 2022) |
| Adsorption | Additional DOC removal | Secondary pollution | (Ma et al., 2021; Rizzo et al., 2019; Zahmatkesh, Amesho, et al., 2022) |
| - <i>Batch sorption</i> | Full scale potential | Need skilled labour | |
| - <i>Continuous fixed-bed</i> | High efficiency | | |
| - <i>Continuous moving bed</i> | Easy process | | |
| - <i>Continuous fluidized bed</i> | Economical | | |
| - <i>Pulsed bed</i> | | | |
| (see section 1.6) | | | |
| Combined treatment | Minimize by-products | Complex process | (Gutiérrez et al., 2021) |
| - <i>MBR (+PAC)*</i> | Highest efficiencies | | |
| - <i>BAC</i> | Combine benefits | | |
| - <i>UV/chlorine (+GAC)</i> | MPs degraded | | |
| - <i>Ozonation + GAC</i> | | | |

*Is usually not implemented as a 'tertiary' treatment

Advanced oxidation processes (AOP) include UV-radiation, fenton and ozonation. What these methods have in common is that radicals are produced as a result of their mechanism. The radicals are also called reactive oxygen species (ROS), such as sulfate or hydroxyl radicals. They are strong oxidants that can rapidly react with organic pollutants (Arvaniti et al., 2022). The pollutant is transformed into smaller and more biodegradable compounds, that possibly can react again with oxidative species so mineralization can take place. The working of AOPs is schematically shown in **Figure 5**. Most common examples of AOPs are given in **Figure 6**. (Trojanowicz, 2020). Some of them are discussed in the context of OMPs management.

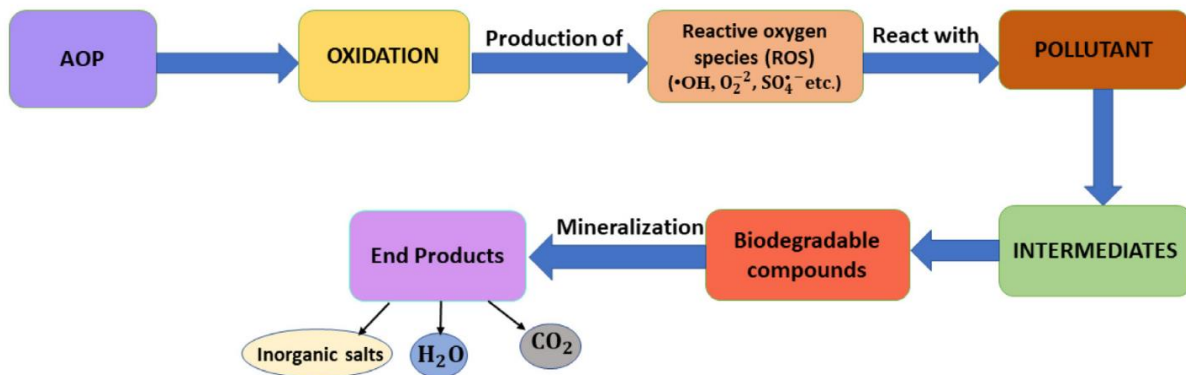


Figure 5 Working mechanisms of the advanced oxidation process, AOP (Kumari & Kumar, 2023)

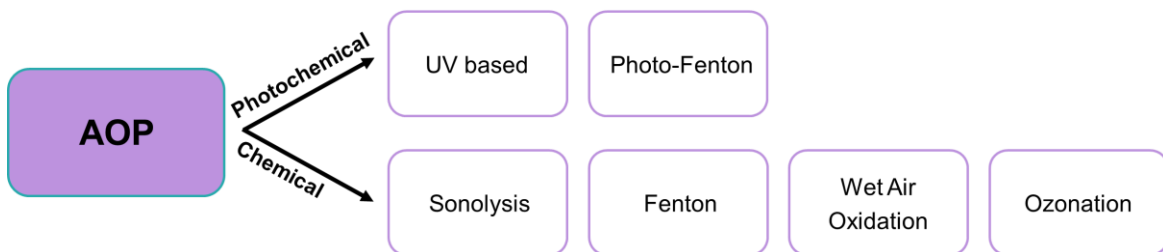


Figure 6 Examples of AOPs subdivided into photochemical and chemical processes

UV-radiation uses UV-light to produce highly reactive hydroxyl radicals ($\bullet\text{OH}$), by which the OMPs are then oxidized. Chlorination uses chlorine, which is converted into oxidative species ($\bullet\text{OH}$, $\text{Cl}\cdot$, $\text{ClO}\cdot$) that creates the ability for organic destruction of OMPs. Chlorination is not an AOP as it does not use oxidation to create ROS. UV-radiation and chlorination are not very efficient when used stand-alone (up to 65% reported), unless high doses are used. However, that would be too costly for the scope of municipal wastewater treatment. The combination UV-chlorine is typically more efficient for removing micropollutants, and lowers the chemical and energy demand (Yin & Shang, 2020). However, the formation of toxic degradation by-products is still concerning with the combination UV-chlorine. Ozonation uses ozone, which reacts with water and produces free oxidizing hydroxyl radicals. The pollutants are then transformed into compounds called ozonation transformation products. These degradation products are smaller and more biodegradable. Next to disinfection, ozonation is also capable of reducing chemical oxygen demand (COD). Ozonation is a very effective method (>90%) for destroying OMPs but residual by-products and high operational energy costs are still aspects of concern (Guilloso et al., 2020; Zahmatkesh, Amesho, et al., 2022; Zahmatkesh, Bokhari, et al., 2022).

Through membrane filtration, very high removal efficiencies are possible. RO and NF are very efficient and widely applied for drinking water treatment, while UF is less efficient in the removal of MPs. Next to these, FO and MD are promising technologies for the removal of OMPs due to their low operating costs and high-quality performance. In terms of efficiency, they might be on the same level as RO and NF, but more research is needed. Drawbacks are: fouling and scaling, expensive high-tech membranes are required and concentrate is a costly secondary pollution (Khanzada et al., 2020; Rizzo et al., 2019).

The feasibility of biological treatment for enhanced degradation of MPs in WWTPs has been recently explored. A moving bed biofilm reactor (MBBR) is a reactor where a biofilm grows on plastic carriers. The working principle of and ‘micropollutants removal’ by MBBR is depicted in **Figure 7**. The different processes, i.e., nitrification/denitrification and organic carbon (OC) removal, occur all together within the biofilm. Because these processes occur simultaneous in one reactor, it is also called a ‘hybrid’ reactor (Mohammadi et al., 2022). Compared to CAS, higher MP removal rates are possible thanks to the high diversity of microorganisms on the carriers (Ahmadi et al., 2023). MBBR is usually not a tertiary treatment but an optimization of the CAS system. MBBR can be recommended when current WWTP need to be improved or when designing new installations for wastewater treatment. This technology is more recent and more advanced for secondary treatment. MBBR has also been investigated as a tertiary treatment after CAS. In this case it is called ‘tertiary MMBR’ and it showed to be an improved addition to the system in the context of CEC removal and degradation (Edefell et al., 2021).

Coagulation and flocculation are processes that are more part of the primary treatment. This group received less interest as MPs adsorbed to the solid sludge are a secondary waste. The sediment is then the pollution problem unless MPs could be purified, which again would be a challenging task (Zahmatkesh, Amesho, et al., 2022).

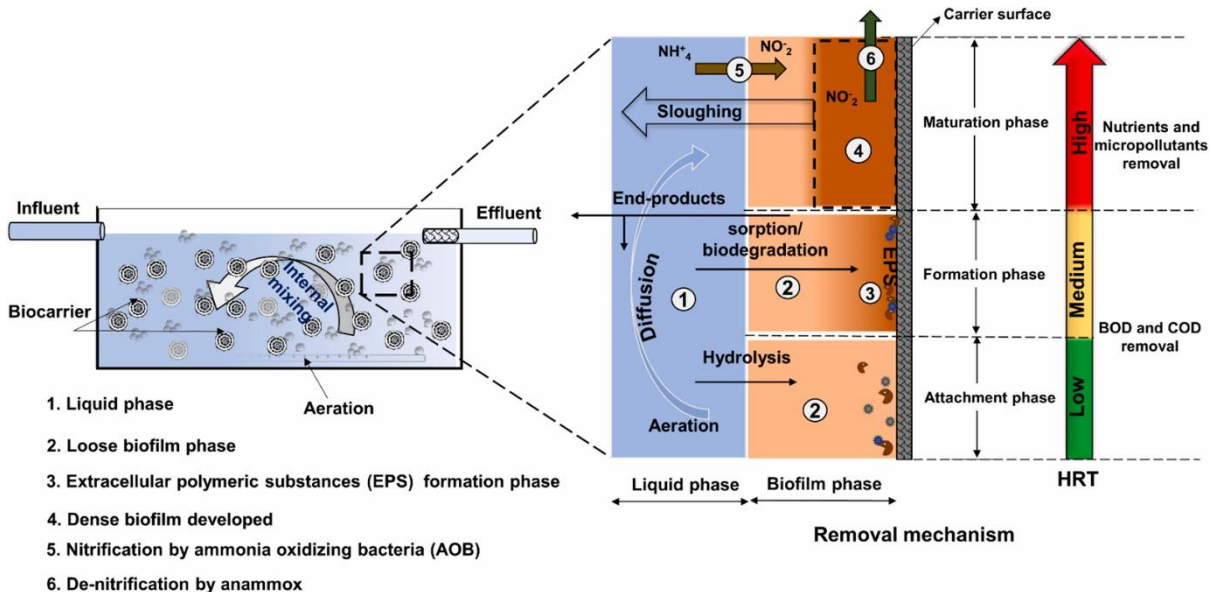


Figure 7 Working principle of a moving bed biofilm reactor, MBBR (Saidulu et al., 2021)

Adsorption is one of the most positively depicted treatment groups in **Table 2**. It features very high efficiencies, with low energy and chemical demands, and is easy to install. Economically, the adsorption method is attracting as installation (CAPEX) and operation (OPEX) costs are rather low. Another benefit is the effective, additional removal of heavy metals (HM) and some dissolved organic matter (DOC). Further, full-scale installations can already be observed at drinking water facilities be transferred to wastewater facilities. Compared to membrane treatment, adsorption has several advantages. First, sorbents can be very abundant when agricultural, food, or industrial wastes are used (Issabayeva et al., 2017), while membranes are products manufactured by complex processes. Another advantage is that activated carbon (AC) has perfect adsorption ability for relatively low molecular mass organic pollutants, making it ideal for tackling micro pollution (Aliakbarian et al., 2015). A downside of adsorption regards the regeneration process. Through regeneration, the concentrated stream of MPs can be removed, but not always recovered. These waste streams are most frequently managed as hazardous waste and then the problem is rather ‘relocated’ than solved. Further being critical, regeneration can sometimes be associated with high energy demands (Ma et al., 2021; Rizzo et al., 2019).

Abatement (%) by several single unit tertiary techniques are listed for 6 CEC in (Rizzo et al., 2019), but is not written out in this paper as abatement strongly depends on the CEC and conditions. Combining some of the above treatment groups can offer many benefits and often results in highest abatements. Examples of how treatment groups from **Table 2** can be combined are discussed in the next section.

1.3.2 Combined technologies for tertiary treatment

A membrane bioreactor (MBR) is an advanced and alternative technology for CAS systems. The combination of biological and membrane treatment provides better-quality effluent with low micropollutant concentrations. It is already widely implemented for water reuse applications. The working principle is shown in **Figure 8**, where OMPs are represented under the name ‘POPs’ or persistent organic pollutants. Fouling is still an issue for this method (Zahmatkesh, Amesho, et al., 2022). Also, a MBR is not a tertiary treatment but rather a more effective substitution for the current WWTPs. MBR is recommended for new installations.

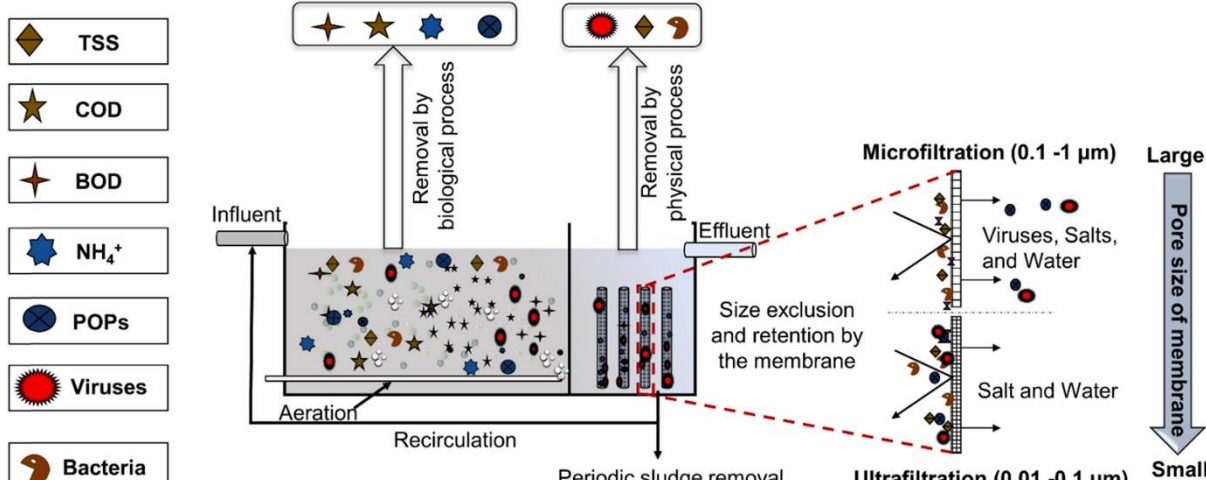


Figure 8 Working principle of a membrane bioreactor, MBR (Saidulu et al., 2021)

Yet another, interesting point is the addition of AC to MBRs. Research has been done to test the addition of powdered activated carbon (PAC) inside the MBR, or GAC as a post-treatment to the MBR. It showed that in either of the technologies, AC effectively enhances the removal of many MPs and at the same time improves the MBR performance (Gutiérrez et al., 2021).

When biological treatment is combined with adsorption, it is called biological activated carbon (BAC). A thin biofilm forms on top of the surface of the activated carbon and allows for the MPs to be, besides adsorbed, also biodegraded. This way, activated carbon can be partially regenerated by the microorganisms while the carbon bed is in operation (Xiaojian et al., 1991). There is no controllable distinction between non-biological and biological AC. However, it is found that pre-ozonation significantly enhances the biological activity on GAC (The BAC Process for Water Purification, 2000). GAC and BAC are shown in **Figure 9**.

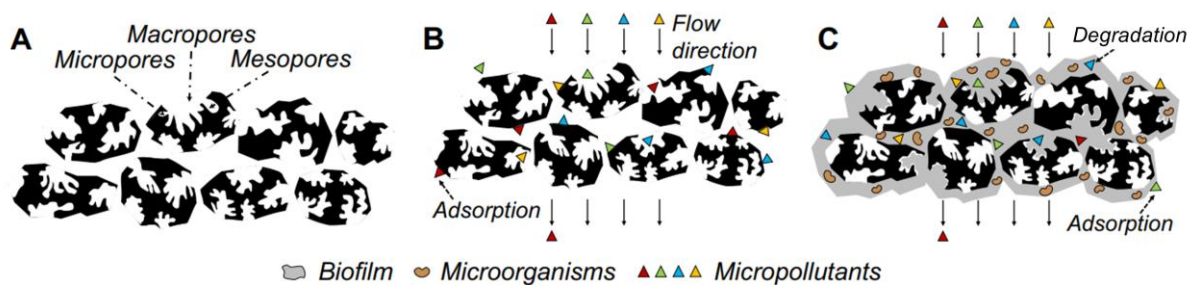


Figure 9 Schematic representation of A: structure of GAC, B: MPs adsorption on GAC, C: BAC (Gutiérrez et al., 2021)

Also combinations between advanced oxidation processes and activated carbon have been investigated, like UV/chlorine – GAC. Degradation by-products were eliminated by the post-adsorption. MPs adsorption rates increased with a factor of 2-3 thanks to the UV/chlorine (Yin & Shang, 2020).

The full-scale project of (Aquafin, 2023), involves a combination of ozonation and GAC as shown in **Figure 2**. Among all tertiary processes discussed, this combination is one of the most interesting and promising. Hence, it is under the loop for implementation in Belgium. It can be easily implemented at the end of the conventional chain without redesign. Ozonation is beneficial in degrading and transforming micropollutants. It also removes compounds that are refractory to adsorption. However, a single ozonation unit demands high energy and can produce toxic by-products. Bromate (BrO_3^-) and NDMA are typical by-products created by ozonation. These are potentially carcinogenic, although this is not proven yet. Post-adsorption by GAC allows using a lower dose of ozone because not all the work needs to be done by this process. This lowers the energy consumption for ozone generation and lowers the by-products formed. Left-over by-products are adsorbed onto the carbon. Another advantage is that competition for adsorption reduces. Namely, dissolved organic carbon (DOC) normally competes with OMPs for the adsorption sites and also causes pore blockage. Ozonation already oxidizes part of the DOM, resulting in less competition. Finally, pre-ozonation enhances BAC formation, stimulating biodegradation onto the GAC. Regeneration will be needed less frequently (Aquafin, 2023; Guillossou et al., 2020). On top of these combination benefits, it is true that the range of removed MPs widens thanks to the two treatment mechanisms together. This can be nuanced with partitioning coefficients LogK_{ow} and LogK_{O₃}. LogK_{ow} indicates the hydrophobicity and therefore affinity of the compound towards AC. LogK_{O₃} indicates its reactivity with ozone. Values for compound-specific coefficients are shown in **Table 3**. Highest removals are observed for compounds with high LogK_{ow} and/or high LogK_{O₃} (Cantoni et al., 2024). This is an interesting way to quantify affinity towards one of the two processes.

Table 3 CEC characteristics for affinity towards AC and ozone (Cantoni et al., 2024)

| CEC | LogK _{ow} | LogK _{O₃} | Function CEC |
|----------------------------|--------------------|-------------------------------|-------------------|
| Acesulfame (ACS) | -0.55 | 1.94 | Sweetener |
| Benzotriazole (BNZ) | 1.3 | 2.38 | UV-filter |
| Diclofenac (DCF) | 4.51 | 6.20 | Anti-inflammatory |

1.4 The adsorption process

Adsorption is a physiochemical interface mass-transfer phenomenon (Ngeno et al., 2022). This definition already gives a hint of its complexity for modelling. Namely, it can be a physical process, a chemical process, or both. The pollutant, also called the adsorbate or solute, is accumulated between two phases. It needs to be clear that the pollutant itself doesn't change phases, but there are two phases involved in the sorption process. In the liquid phase, the pollutant is dissolved. When the pollutant is in the solid phase, also known as the sludge phase, it means that the pollutant is adsorbed onto the solid (Mohammadi et al., 2022). The adsorbent, e.g. activated carbon, is a porous material with both outer and inner surface that is exposed to the adsorbates. On the surface, the active sites are the places where the solute can directly adsorb onto. However, the pollutant first needs to travel a pathway from the aqueous media (liquid phase) to the active sites (solid phase). In this pathway, different mass transfer and diffusion mechanisms take place. Diffusion is defined by the movement of particles due to a concentration gradient. Once the active site is reached, different adsorption mechanisms are possible: chemisorption, physisorption or both. Chemisorption include ionic interactions or the formation of chemical bonds between the sorbate and sorbent molecules. Physisorption include Van der Waals or π - π interactions. These adsorption mechanisms influence the way the pollutants are structured onto the surface: monolayered or multilayered. Physisorption, such as Van der Waals interaction, mainly contributes to multilayer adsorption. Chemisorption, such as hydrogen bonding or the formation of strong bonds, mainly contributes to monolayer adsorption. It is the result of interaction between the adsorbate and functional groups on the adsorbent surface (Aliakbarian et al., 2015; Ngeno et al., 2022; Wang & Guo, 2023). An illustration of the adsorption process is shown in **Figure 10**.

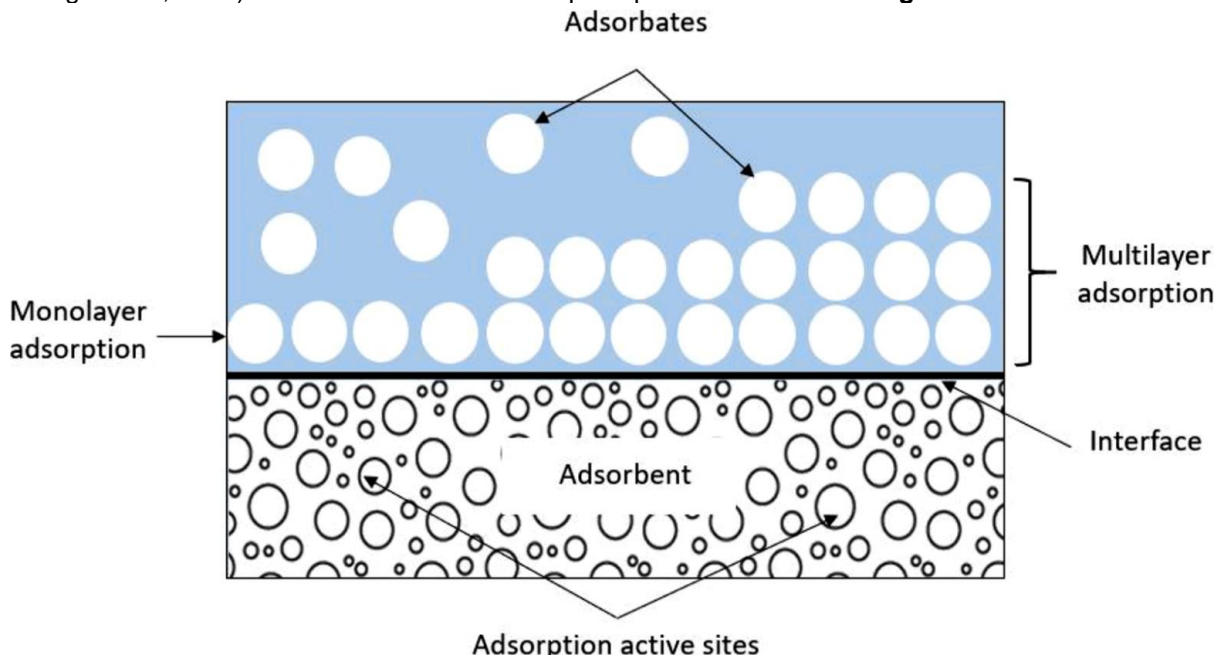


Figure 10 Illustration of the adsorption process (Ngeno et al., 2022)

When modelling the adsorption process, it is important that the diffusion mechanisms and adsorption mechanisms are taken into consideration as good as possible. Although this is very complex and results in more theoretically grounded and thus more reliable models. In the past, models not always included these theoretical basis as they were built for specific purposes, for example the removal of phenolic compounds from olive mill wastewater (Aliakbarian et al., 2015). However, since the focus is on municipal wastewater, various pollutants with various diffusion and adsorption mechanisms exist. Thus, for the application in this thesis a more comprehensive model will be required.

1.5 Types of adsorbents

An overview of different adsorbent groups, distinguished based on their origin or nature, is shown in **Figure 11**. Each group is provided with some of the most important adsorbents and their adsorption capacity for phenol. Phenol was taken as the standard compound to be able to compare the different adsorbents. The values for phenol are extracted from the review paper of (Issabayeva et al., 2017). It should be noted that, next to organic micropollutants such as phenols, there are many other OMPs and inorganic MPs. Examples of inorganic micropollutants are heavy metals, toxic metal ions and inorganic salts such as fluorides. Also, relative values for adsorption capacity can differ dependent on the conditions. The range of influent concentration is also a factor that determines which adsorbent suits the best (Issabayeva et al., 2017).

Adsorption onto granular activated carbon (GAC) was chosen by the United States Environmental Protection Agency (US-EPA) as the best available technology for the treatment of many regulated organic pollutants (Westerhoff et al., 2005). Thanks to its good properties, GAC is still one of the most widespread technologies in drinking water treatment (Piazzoli & Antonelli, 2018). However, there exist many other possibilities next to GAC, each having its own pros and cons.

Adsorbents

| Carbonaceous adsorbents | Clay and mineral-based adsorbents |
|---|-----------------------------------|
| | Capacity (mg/g) |
| • Commercial AC <ul style="list-style-type: none">– GAC 350– PAC 303 | – Modified bentonite 333 |
| • Agri waste-based AC <ul style="list-style-type: none">– Coconut shell AC 206-240– Sugar cane bagasse 33– Tea leaves 9,49– Rice husk (ash) 0,0022-14,38 | – Red mud 59,2 |
| • Food waste-based AC <ul style="list-style-type: none">– Corn cob AC 232-340– Corn cob 177,6– Chitosan (seafood waste) 59,74 | – Surface modified zeolite 37,92 |
| • Industry waste-based AC <ul style="list-style-type: none">– PET 162-278– Coal slug 63,78 | – Natural zeolite 34,5 |
| • Novel adsorbents <ul style="list-style-type: none">– MAA-coated NPs 950– Nanoparticles (NPs) 550– HMCSs 207,8– Nanotubes 1,1-64,6 | – Natural clay 15 |
| Polymer-based adsorbents | Capacity (mg/g) |
| – BMS 1000 | – Nanotubes 1,1-64,6 |
| – XAD-16 141,17 | – MAA-coated NPs 950 |
| – NJ-8 136,9 | – Nanoparticles (NPs) 550 |
| | – HMCSs 207,8 |

**Figure 11 Overview of adsorbent groups with some of the most important adsorbents listed.
The values for adsorption capacity are given for phenol as the adsorbate compound
(Issabayeva et al., 2017)**

Four groups are separated based on their origin or nature and will be shortly discussed. It also must be noted that adsorbents can be modified to improve properties. The more is modified, the better the adsorption capacity but also the higher the price. Three groups can be distinguished (Patel, 2019):

- Semi-synthetic adsorbents: natural materials undergo chemical and physical activation to develop a highly porous structure. This group includes activated carbon and seems to find a very good balance between costs and efficiency
- Natural adsorbents such as unmodified clay and mineral-based adsorbents form the second and most economical group. It is a sustainable option as no modification is needed and there is high abundance. However, they typically come with low adsorption capacities
- Synthetic adsorbents undergo advanced laboratory processes to improve adsorption capacity, but the price and sustainability of this group are the main concerns. Manufacturing is relatively costly. Polymer-based and novel adsorbents belong to this group

Carbonaceous adsorbents are carbon-based adsorbents and include activated carbon (AC in **Figure 11**). AC is well-known for its good adsorption ability for relative low molecular mass organic compounds, its good physical and chemical properties, porous structure, large specific area and availability of surface functional groups for binding (Aliakbarian et al., 2015; Issabayeva et al., 2017; Šerban et al., 2023). The activation process and different sources for AC are further discussed below.

Activation can be done physically or chemically. Activation is typically done through pyrolysis. In this process, organic material is decomposed by heating in the absence of oxygen. This way, the material is converted to carbon. Two important variables in this process are heating rate and duration. Chemical activation requires the addition of a chemical to the material that will ultimately modify the surface groups. These surface functional groups will help improve the adsorption characteristics of the material. Chemical activation requires less energy. Also, short reaction times are possible. A drawback is that the used chemicals can be environmentally hazardous. Physical activation includes the addition of oxidizing agents like steam, carbon dioxide (CO_2) and air. The activator used is more environmentally friendly compared to chemical activation, but the yield might be lower (Ngeno et al., 2022).

Commercial AC is a term that refers to AC gained from conventional, fossil sources. By far the oldest adsorbent ever used is charcoal. It has been applied widely in drinking water facilities. In the past, the aim was to get clean water so more people would have access to drinking water. There was not yet an incentive for sustainable design. Charcoal and later petroleum coke and lignite are products originated from fossil sources and are not the most eco-friendly. Adsorption capacities for phenol on commercial granular and powdered activated carbon are 350 and 303 mg/g respectively (Issabayeva et al., 2017).

The differentiation between granular activated carbon (GAC) and powdered activated carbon (PAC) is made based on its particle size. They are both created from conventional or unconventional carbon-based sources, but PAC is the more refined version. GAC has larger particle size (granules) and smaller external surface. However, it can be easily reactivated through regeneration. Another advantage is the high porosity of the granules, which enhances mass transfer of MPs significantly. PAC has finer particles and is mainly used in batch reactors, where it can flexibly be dosed. The capital cost of PAC is two times lower than GAC. However, regeneration is intensive and usually not done. Regularly replacement will lead to higher operational costs. Another disadvantage of PAC is that it causes sludge to accumulate and leak through treatment filters (Brandt et al., 2017, p. 10; Issabayeva et al., 2017).

As said, activated carbon can also be generated from unconventional sources which are more renewable. Agricultural, food and industrial wastes are very abundant and can be converted into effective AC. Adsorption capacities for phenol are listed in **Figure 11** from high to low. Although their efficiency is not very stable, some can reach almost the same as commercial activated carbon. Big advantages compared to commercial AC is their high and local abundancy and low production costs. This can give these semi-synthetic adsorbents a very good balance between sustainability and efficiency. Corn, being a globally produced crop, is a good example of a sustainable precursor. Corn cob is widely abundant and, when activated, reaches adsorption capacities up to 340 mg/g. Coconut shells AC also has significant adsorption capacity, up to 240 mg/g, and can be a sustainable option near these agricultural areas. Also industry has carbon-based wastes such as polyethylene terephthalate (PET). Plastic waste is clearly a major global environmental problem and PET seems to have high carbon content. PET waste can be converted into activated carbon through a chemical, physical or other combined activation processes. For the adsorption of phenol, a maximum adsorption capacity of 278 mg/g has been obtained (Issabayeva et al., 2017; Sharifian & Asasian-Kolur, 2022).

Clay and mineral-based adsorbents form the most natural group of adsorbents as they are directly available in nature. However, these adsorbents can also be modified to improve their adsorption properties. These adsorbents are not carbon-based. Zeolite is a mineral with medium capacity for phenol, but is getting more interest thanks to its easy regeneration. Regeneration also plays a significant role in determining the strengths of an adsorbent choice. Bentonite is a clay-containing sorbent with exchangeable cations. Naturally, its adsorption capacity is low but if it is treated and activated, up to 333 mg phenols/g can be adsorbed, which is close to the 350 mg/g by GAC (Issabayeva et al., 2017).

Polymer-based adsorbents are non-carbonaceous, economically promising adsorbents that show good properties for the removal of organic micropollutants. The main concern is the harm of these materials to the environment and the harm of the polymerization process, although it can be available as a waste. The polymers can show outstanding (up to 1000 mg/g) adsorption capacity for phenol. They have a specific, small pore size distribution and can easily be regenerated (Issabayeva et al., 2017).

A fourth group is the group of **novel adsorbents**. Here, novel materials and techniques are used to obtain optimal adsorption capacities. They undergo a variety of thermal and chemical modifications and mostly on lab-scale. Just as polymer-based, these synthetic adsorbents can have a high cost of production, disposal and potential pollution to the environment. An example is the manufacture of nanotubes with an adsorption capacity for phenol around 64,6 mg/g. This can be a novel continuation of the process where PET waste is activated. Other novel processes are the synthesis of nanoparticles (NPs) and their coating, which again leads to outstanding adsorption capacities, up to 950 mg phenol/g of adsorbent (Issabayeva et al., 2017; Sharifian & Asasian-Kolur, 2022).

A last division of adsorbents is based on polarity (Ngeno et al., 2022):

- Polar adsorbents are hydrophilic and typically show a higher affinity to polar substances such as alcohols. Clay and mineral-based adsorbents such as zeolite and bentonite typically are polar adsorbents
- Non-polar adsorbents are hydrophobic and show a higher affinity to non-polar substances such as oil and hydrocarbons. Carbonaceous and polymer-based adsorbents typically are non-polar adsorbents

1.6 Types of adsorption set-ups

Various techniques exist that make use of the adsorption method. Explanation, advantages and disadvantages are listed in **Table 4** that is derived from the study of (Patel, 2019). The differences are mainly based on the flow of the adsorbent and adsorbate. Batch adsorption is a non-continuous process in which adsorbent and adsorbate are mixed, and after equilibrium the adsorbent is removed by drawing off. It is only possible with low amount of adsorbent and low pollution load. Therefore, this technique refrains from industrial-scale applications. The same is true for pulsed bed adsorption, in which the exhausted adsorbent is periodically removed from the bottom while new or regenerated adsorbent is added on top (Sookkumnerd, 2019). The other sorption processes are called continuous because the influent flow can be fed continuously through the bed. The term continuous gives no indication about the regeneration, this can be periodically. Typically, also larger amounts of adsorbent are used here. Continuous sorption processes can be used for higher amount of wastewater with higher pollution loads and are therefore more interesting in the application of municipal wastewater. Among them, continuous fixed-bed adsorption is depicted as a suitable technique. It doesn't require large investment or large area but can be implemented at large scale (Patel, 2019, 2022).

Table 4 Introduction, pros and cons for various adsorption systems (Patel, 2019)

| Adsorption system | Introduction | Pros + | Cons - |
|--|---|---|---|
| Batch sorption | Adsorbent and adsorbate are mixed in diluted solution at constant volume | Easy and cheap Desired for research | Non-continuous For small quantity of wastewater and minimum pollution load Usually not industrialized Adsorbent removed by simple filtration |
| Continuous fixed-bed sorption | Adsorbate continuously flows through the adsorbent bed at constant rate | Easy and cheap Continuous For higher quantity of wastewater and higher pollution load Widely used for industrial application | Attrition (wear particles) Feed channelling Dead zones |
| Continuous moving bed sorption | Continuously flowing adsorbate and also adsorbent are in motion | Continuous good contact with fresh adsorbent | Complicated & expensive Large amount of adsorbent required Continuous regeneration of adsorbent essential |
| Continuous fluidized bed sorption | Adsorbate is in contact with fluidized bed of adsorbent | Continuous For higher quantity of wastewater and higher pollution load Automatically controllable Industrial scale | Complicated & expensive Rapid mixing leads to non-uniform residence time |
| Pulsed bed sorption | Adsorbate is in contact with the same piece of adsorbent in bed, until effluent quality exceeds limit | Easy and cheap Automatically controllable Low adsorbent dosage required Optimal regeneration time | For small quantity of wastewater and minimum pollution load |

1.7 Adsorption equilibrium

As explained in **paragraph 1.4**, adsorption is a process where the solute, also called adsorbate, accumulates between two phases: the liquid phase and the solid phase. The adsorbate is adsorbed onto the active sites of the solid surface, i.e. any external or internal surface of the GAC. As the amount of activated carbon in the bed is limited, also the number of active sites is limited. Not all pollutants are removed but an equilibrium is obtained. The adsorption process involves both sorption and desorption. Equilibrium is reached between concentrations in the liquid phase and in the solid phase.

Equilibrium behaviour of a solute in GAC is described through the adsorption isotherm. The isotherm is determined by conducting a conventional static method in a closed system. A prior determined amount of carbon is added in a beaker together with polluted water. The water contains single-solute pollution with a known initial concentration. Equilibrium is reached when the micropollutant is long enough in contact with the adsorbent. The adsorption and desorption are now equal in rates. Solute concentration is carefully measured after equilibrium. The two important equilibrium values are:

- q_e = [pollutant] in solid phase at equilibrium (mg/g AC), also called adsorption capacity
- C_e = [pollutant] in liquid phase at equilibrium (mg/L bulk liquid)

These values are determined for different initial solute concentrations, and the relationship is plotted. The relationship is called the equilibrium isotherm and can be seen in **Figure 12**. Due to complexity of adsorbate – adsorbent interactions, diverse shapes of isotherms exist for diverse adsorption systems, see **Figure 12(a)**. This is why, for the respective micropollutant and GAC, it is desired to determine equilibrium behaviour experimentally. Examples of L-shape isotherms are schematically shown in **Figure 12(b)**. Differences can be attributed to various micropollutants, for example. The red isotherm seems to be superior because adsorption capacity is highest at any dosage.

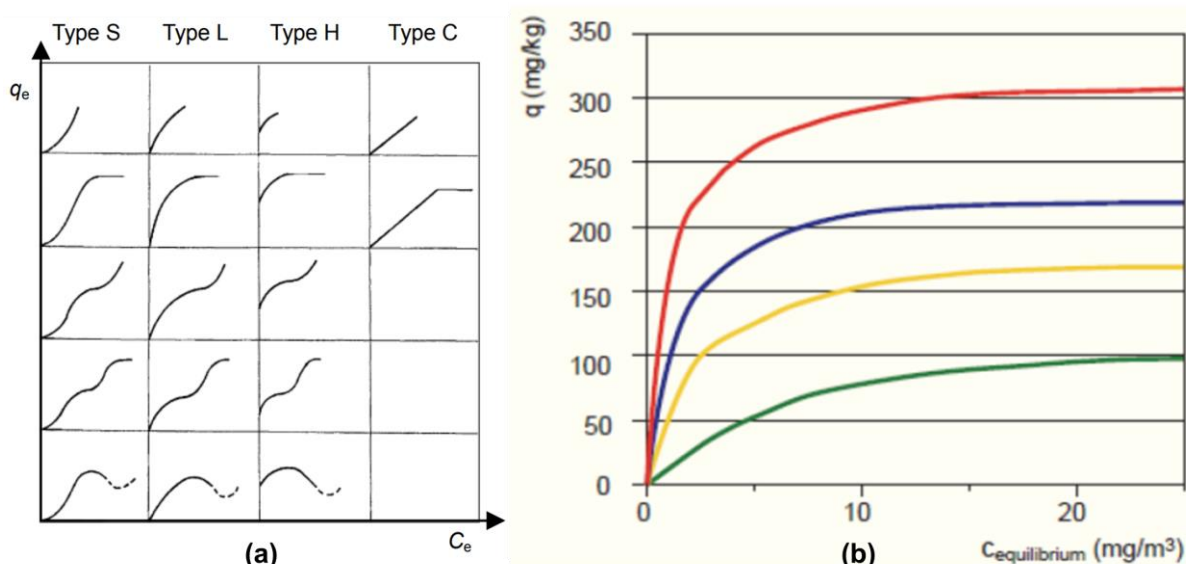


Figure 12 Equilibrium isotherms: (a) classification according to shape, (b) shape L examples, each colour is a different sorption system (Vanoppen, 2023; Xu et al., 2013)

It is assumed that at the surface of the adsorbent, the solid-phase solute concentration (amount of solute adsorbed) is in equilibrium with the liquid-phase solute concentration (Jarvie et al., 2005).

1.8 Adsorption kinetics

The adsorption kinetics describe the whole movement process of the solute inside the fixed-bed adsorption column. There is more than the adsorption reaction itself that is described in **section 1.7**. Only considering adsorption onto the active sites is not sufficient when modelling GAC columns. There is a sequence of steps preceding adsorption, from which duration of each step can be relevant to take into consideration. Different steps, next to adsorption itself, are schematically represented in **Figure 13**.

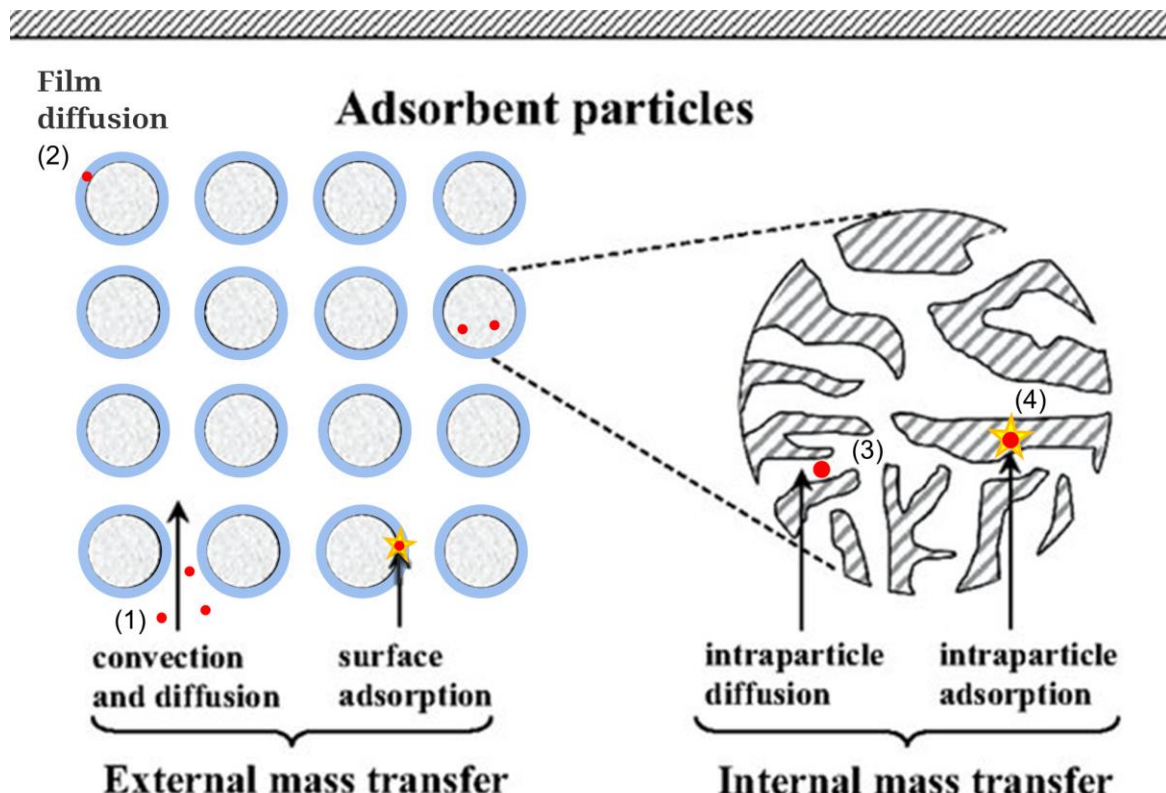


Figure 13 Different steps for adsorption kinetics (1) (2) (3) and reaction (4) occurring during fixed-bed adsorption (Zhou et al., 2016). Edit for liquid instead of gas.
Blue = particle film

The following are basic mechanisms that are important in an adsorption column, see **Figure 13**. There are four steps the solute undergoes when eliminated by adsorption and any of them can be rate-limiting (Xu et al., 2013).

- (1) **Liquid phase mass transfer** including convective mass transfer and molecular diffusion
- (2) **External film diffusion** between liquid phase and exterior surface of the adsorbent. This mass transfer occurs in the 'boundary layer', which is the surrounding of every adsorbent particle inside the GAC bed
- (3) **Intraparticle diffusion** which consist of pore diffusion and surface diffusion. Pore diffusion is the mass transfer of the solute in the pore volumes of the GAC particle. To be specific, it is a general name for molecular and/or Knudsen diffusion. Molecular diffusion mainly takes place in macropores and results from collisions between molecules. Knudsen diffusion dominates in micropores due resulting from collisions between molecules and the pore wall. Surface diffusion

is the movement of the solute that hops between adsorption sites. Intraparticle diffusion strongly depends on concentration and size of the pollutant (S. Sharma et al., 2023).

It is assumed that, at the adsorbent surface, the solid-phase solute concentration is in equilibrium with the liquid-phase solute concentration (Jarvie et al., 2005). Locally, the liquid-phase concentration at the adsorbent particle surface is related to the adsorption capacity at the particle surface by the equilibrium relationship (Inglezakis et al., 2019). Therefore, the isotherm is a relevant aspect here. It gives information about the amount of solute that can adsorb when the concentrated stream is near to the surface and this is compound-specific.

- (4) **The adsorption- desorption reaction** on the active site (physical / chemical, monolayered) or onto other particles (physical, multilayered). The adsorption itself can take place directly onto the external surface of an AC granule, or after intraparticle mass transfer onto the internal surface of an AC granule. This is also illustrated with a yellow star in **Figure 13**

Figure 14 demonstrates the intraparticle diffusion mechanisms more in detail.

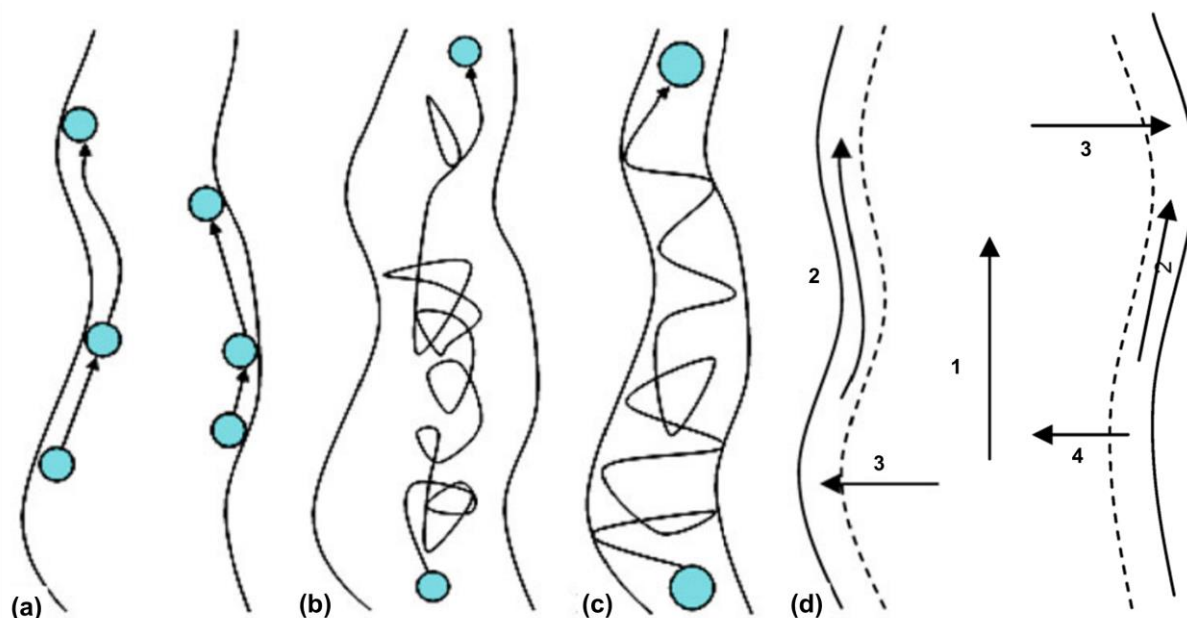


Figure 14 Intraparticle diffusion mechanisms: (a) surface diffusion, (b) pore diffusion, (c) pore diffusion with significant Knudsen diffusion, (d) combination of 1 pore diffusion, 2 surface diffusion, 3 adsorption, 4 desorption (Xu et al., 2013)

1.9 The breakthrough curve

The sequence of adsorption in a continuous fixed-bed adsorption column is illustrated in **Figure 15**. Adsorption, i.e. mass transfer, does not occur in the entire column simultaneously. If the influent is coming from above, the activated carbon in the top layer of the fixed-bed column will initially adsorb all the micropollutants. Meanwhile, the bottom of the column receives already well treated influent with low concentration of OMPs, leading to a very low mass transfer.

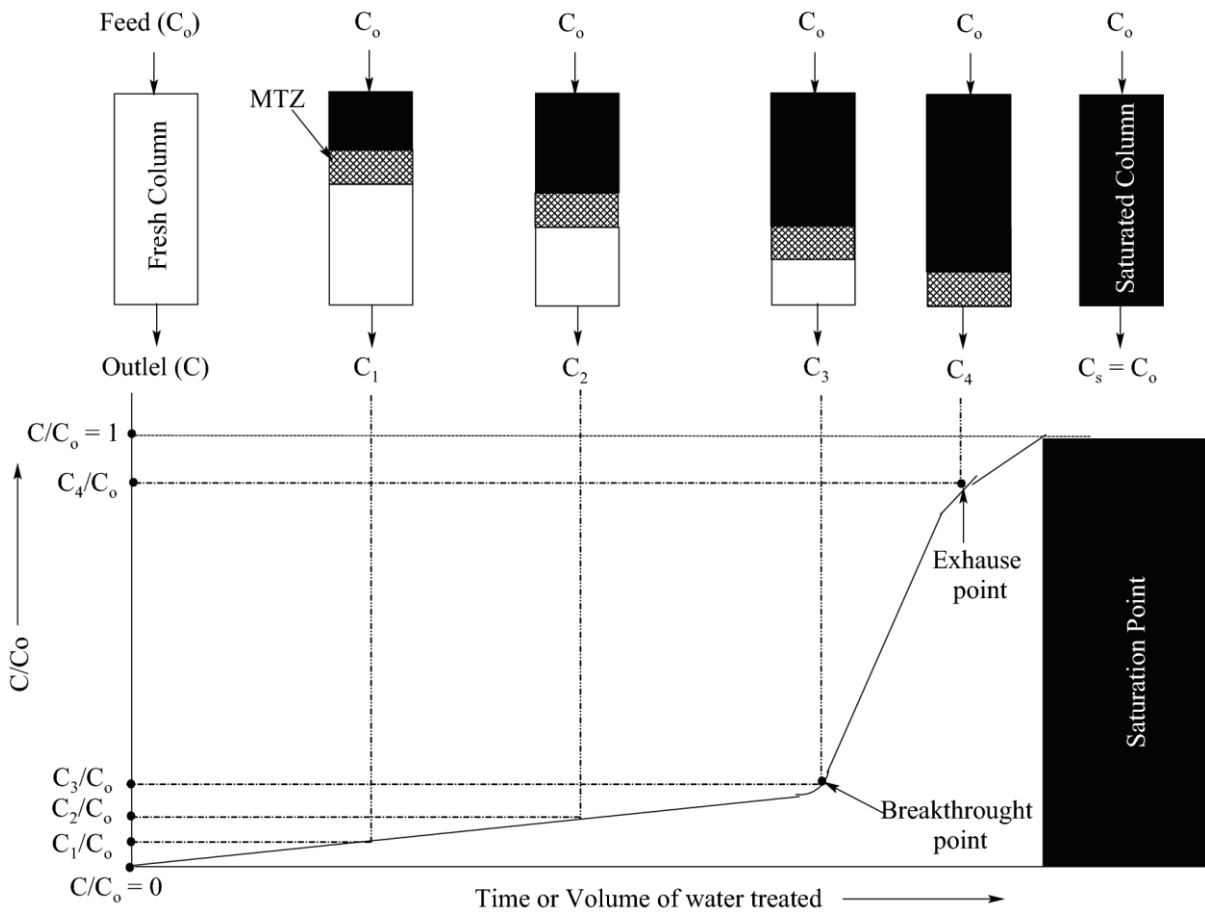


Figure 15 Representation of adsorption in a fixed-bed column and the link with breakthrough curve (Patel, 2019)

As said, initially, there is fresh carbon on top that is in contact with non-treated effluent and causes the driving force ($C_o - C_e$) to be highest on top of the column. C_o is the concentration of pollutant in the influent. Above in the column, no adsorption has already been done and $C = C_o$. At the bottom, initially there is no driving force because the influent is already treated by the upper part and doesn't contain pollutants anymore. However, the above part gets saturated after some time and the zone with highest driving force will move downwards. The region where mass transfer occurs depends on time and space and is called the mass transfer zone (MTZ). It is illustrated as the dotted area in **Figure 15** and is preceded by a saturated carbon zone (black area) and followed by fresh carbon (white area).

A breakthrough curve (BTC) is a plot of the fixed-bed column effluent concentration as function of time or volume of water treated. Initially, with a fully fresh column, the effluent concentration is perfectly treated and ideally contains zero pollutants. After a while, due to saturation, the effluent concentration increases. Above the breakthrough point, the effluent concentration is considered too high for successful removal. This can be 5% of the influent concentration, dependent on the desired effluent quality. From then, typically concentrations increase more rapidly and at the point of exhaustion, the bed is considered exhausted. The effluent concentration is only 5% lower than the highly concentrated influent. At perfect saturation, there is absolutely no adsorption anymore (Sabri & Abbood, 2019).

2 ADSORPTION ON ACTIVATED CARBON: BREAKTHROUGH CURVE MODELS

This chapter explains what breakthrough curve models are, what opportunities they can deliver, why different models exist and which ones make chance for modelling tertiary GAC treatment in WWTPs. The scope is limited to single-solute adsorption onto non-biological GAC in fixed-bed columns.

2.1 Opportunities and challenges

A breakthrough curve (BTC) is crucial information for the design and operation of real-life adsorption systems tackling OMPs in municipal wastewater. With the BTC, one can make conclusions about the adsorption performance, how long before regeneration is needed, what is the removal efficiency at any time, etc. However, making BTCs for a variety of compounds in a variety of conditions is a costly operation. Applying for municipal wastewater, this requires many pilot-scale experiments. Models that could trustfully predict BTCs for all these different scenarios could save a lot of time and money. It would help to predict in which scenarios one gets maximum removal efficiency, adsorption capacity, and predict bed replacement intervals. This facilitates to figure out if GAC is a viable technology for full-scale advanced wastewater treatment. Hence, there is opportunity to meet emission thresholds for micropollutants in the future. In the coming years, the need for optimised treatment systems will only increase as legislation around micropollutants will get more strict (J. Burkhardt et al., 2022).

A first challenge regards the complexity of the WWTP's influent: municipal wastewater. Municipal wastewater is a complex stream containing many different micropollutants in highly varying concentrations. It is not only the concentration of MPs itself that vary over time. The WWTP's influent composition is uncertain and variable. For example, dissolved organic matter (DOM) is important to address as it competes with MPs, but it is variable and hard to quantify. Environmental conditions such as the temperature and pH also change continuously. Also the flow rate of the incoming stream and weather conditions change unpredictably over time.

A second challenge can be seen as a consequence of the first one. Because adsorption systems for micropollutants are new and complicated, the gap of information in literature remains big. Models have been developed but rarely used for simulating full-scale fixed-bed GAC columns treating municipal wastewater. Contrary, most of the models are limited in scope and complexity. For instance, modelling the adsorption of phenolic compounds from olive mill wastewater (Aliakbarian et al., 2015). Such a model can only be used for a limited situation and would fail in describing others (Xu et al., 2013). Another reason why research is not highly developed for this topic is the lack of data on MPs in wastewater. Measuring trace concentrations is time-consuming and costly. Also, it is only recently that measuring becomes more relevant as regulatory thresholds evolve.

The model quickly becomes complex when considering all variabilities in the context of municipal wastewater. The more complex the model, also the more equations and the more parameters that are needed. However, it is hard to calibrate a model with too many parameters. The sum of uncertainties for all these parameters would be too high. This also depends on how much information there is about the parameters. There is no problem if all parameters are perfectly known but mostly high efforts are needed to determine or calculate them. It is said that applicability of large adsorption models is restricted due to the low availability of internal transport parameters (Worch, 2008). A balance need to be found between accuracy of the process description and reliability of the model results.

2.2 Components of fixed-bed BTC models

A breakthrough curve (BTC) model is a model containing a set of partial differential equations, and usually consists out of three components (Worch, 2008; Xu et al., 2013):

- The differential mass balance equation
- The uptake rate equation(s) describing adsorption kinetics
- The equilibrium relationship isotherm equation (scope: single-solute)

This division is necessary to fully describe the four steps the micropollutant undergoes in a fixed-bed adsorption column, as explained by **Figure 13**. The uptake rate depends on how fast mass transfer and diffusion occurs in the pathway to the adsorption sites. The isotherm is useful at the adsorbent surface, where solid- and liquid-phase concentrations are assumed to be in equilibrium (Jarvie et al., 2005).

2.3 Equilibrium relationship: isotherm equations

This paragraph shows an overview of (common) isotherm equations that can be used in fixed-bed BTC models. The purpose is to simulate equilibrium behaviour as good as possible. As said, it is desired that equilibrium is studied experimentally, if not done before, because every solute-sorbent interaction is different. In the model, equilibrium is represented by an isotherm equation. This is a simple function with two or more isotherm parameters. When reliable experimental equilibrium data is available, the isotherm equation can be fitted to this dataset. Numerous isotherm equations have been developed in the past to mimic the diverse shapes that exist in practice. The Freundlich and Langmuir equations are simple and most frequently applied for single-solute equilibrium simulation (Aliakbarian et al., 2015).

Some isotherm equations are based upon monolayer (chemical) adsorption, other on multilayer (physical) adsorption. When Van der Waals interaction dominates the mechanism, the adsorption is mainly a multilayered process as solutes can also physically attract each other. When the mechanism is mainly dominated by hydrogen / strong bonding with functional groups on the surface, adsorption is monolayered (Wang & Guo, 2023). The two adsorption mechanisms are illustrated in **Figure 16**. Names of common isotherm equations for heavy metals are shown in **Figure 17**.

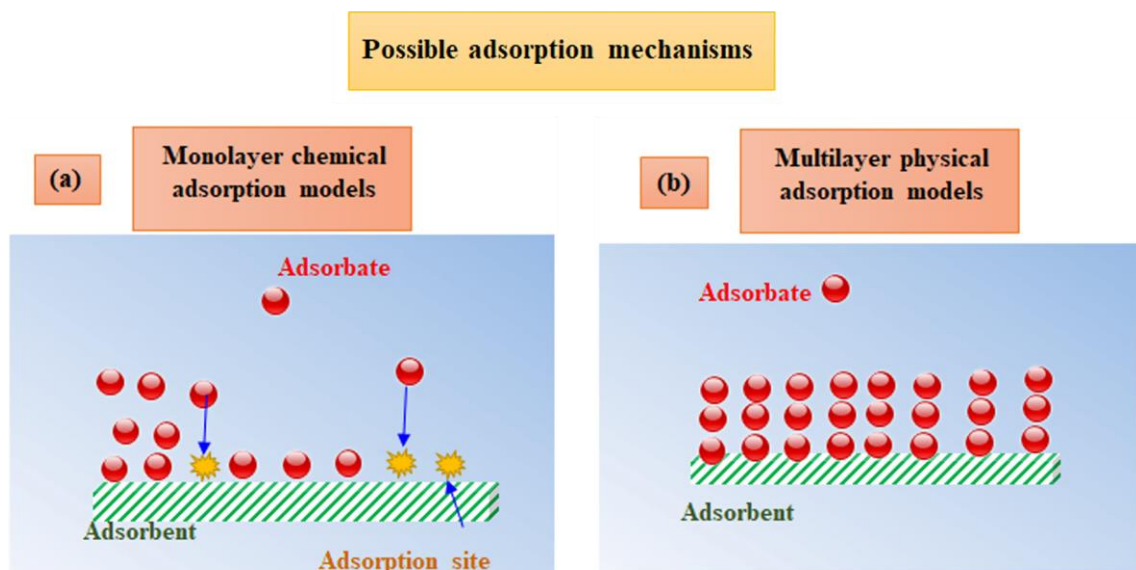


Figure 16 Theoretical adsorption mechanisms on the adsorbent surface (Saleh, 2022)

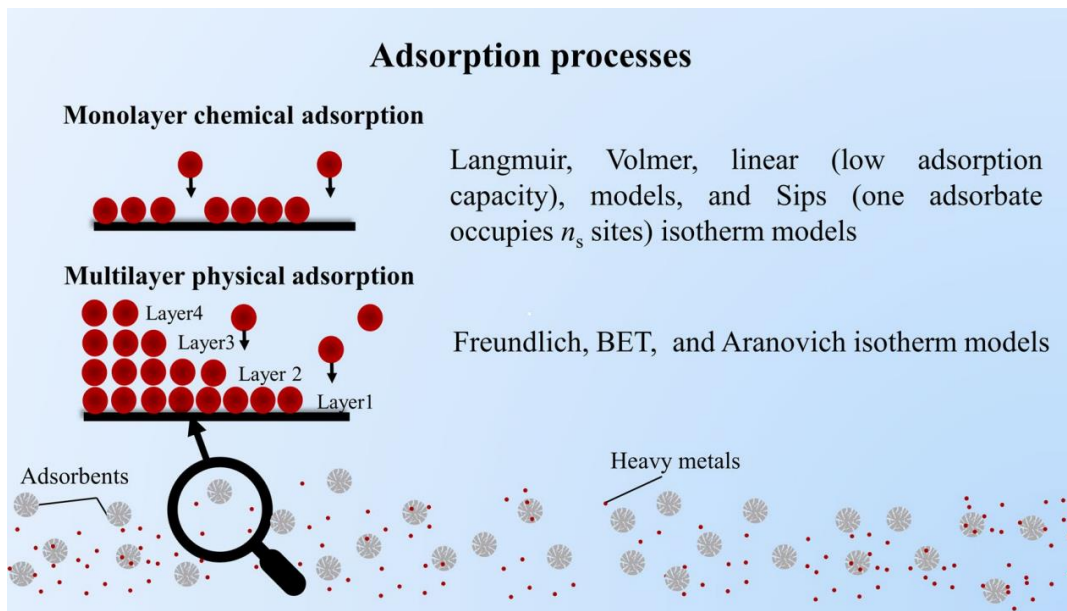


Figure 17 Adsorption mechanisms and corresponding adsorption isotherm models (Wang & Guo, 2023)

2.3.1 Freundlich isotherm equation

The nonlinear Freundlich equation is one of the most widely used for describing equilibrium. It covers both multilayer and monolayer adsorption with 50 % active site occupation (Wang & Guo, 2023). The isotherm assumes the following:

- The surface is heterogeneous: adsorption energy varies as a function of the surface coverage due to variation in adsorption heat. On the heterogeneous surface, affinities between adsorbent and adsorbate show an unstable distribution (Aliakbarian et al., 2015; Ţerban et al., 2023)

The equilibrium parameters follow a relationship that is mathematically described in equation (1) or linearized in equation (2) (Aliakbarian et al., 2015; Ţerban et al., 2023; Vanoppen, 2023).

$$q_e = K_F * C_e^{1/n} \quad (1)$$

$$\ln(q_e) = \ln(K_F) + \frac{1}{n} \ln(C_e) \quad (2)$$

In which:

- q_e = equilibrium solid-phase mass of solute per mass of sorbent (mg_{solute}/g_{carbon})
- C_e = equilibrium solute concentration in bulk liquid (mg_{solute}/L)
- K_F = Freundlich coefficient ((mg/g)*(L/mg)ⁿ)
- $1/n$ = Freundlich exponent (-)

K_F is a constant for a given sorbate related to the sorption capacity and $1/n$ is a constant for a given sorbent related to the sorption intensity (Aliakbarian et al., 2015; Vanoppen, 2023). The Freundlich exponent accounts for adsorption site energy distribution (Jarvie et al., 2005). The Freundlich isotherm is an empirical equation and critics claim it has lack of physical meaning (Saleh, 2022).

2.3.2 Langmuir isotherm equation

The Langmuir equation is also popular in isotherm studies and falls under the class of chemical isotherms. Chemical isotherms consider monolayer adsorption, which means that all molecules are localised in the adsorption sites. The equation is not empirical but theoretical and therefore it has more physical meaning for this context (Wang & Guo, 2020). Assumptions when applied, are:

- The surface is homogeneous: all adsorption sites are energetically identical. The surface's adsorption sites have uniform energies of adsorption without transmigration of adsorbate in the pores of the adsorbent surface (Aliakbarian et al., 2015; S. Sharma et al., 2023)
- There are no lateral interactions between adsorbed molecules: interaction between solutes is ignored (S. Sharma et al., 2023; Wang & Guo, 2023)

These assumptions are thus true for chemical adsorption, also called chemisorption (S. Sharma et al., 2023). The equilibrium parameters follow a relationship that is mathematically described in equation (3) (Aliakbarian et al., 2015; Wang & Guo, 2020, 2023)

$$q_e = \frac{q_m K_L C_e}{1 + K_L C_e} \quad (3)$$

In which:

- q_e = equilibrium solid-phase mass of solute per mass of sorbent (mg_{solute}/g_{carbon})
- C_e = equilibrium solute concentration in bulk liquid (mg_{solute}/L)
- K_L = Langmuir constant, ratio adsorption and desorption rates (L/mg)
- q_m = maximum adsorption capacity (mg_{solute}/g_{carbon})

When the Langmuir model is applied, often an indicator is used to evaluate if the adsorption can be considered favourable. The adsorption is favourable if the separation factor is situated between $0 < R_L < 1$. This constant can be calculated by equation (4) (Serban et al., 2023; Wang & Guo, 2023).

$$R_L = \frac{1}{1 + K_L C_0} \quad (4)$$

In which:

- R_L = separation factor (-)
- C_0 = initial solute concentration in bulk liquid (mg_{solute}/L)
- K_L = Langmuir constant (L/mg)

2.3.3 Other isotherm equations

Other isotherm models in **Figure 17** are well explained by (Wang & Guo, 2020) and (Saleh, 2022, p. 4). A summary and general classification of adsorption isotherms are represented in **Figure 18**.

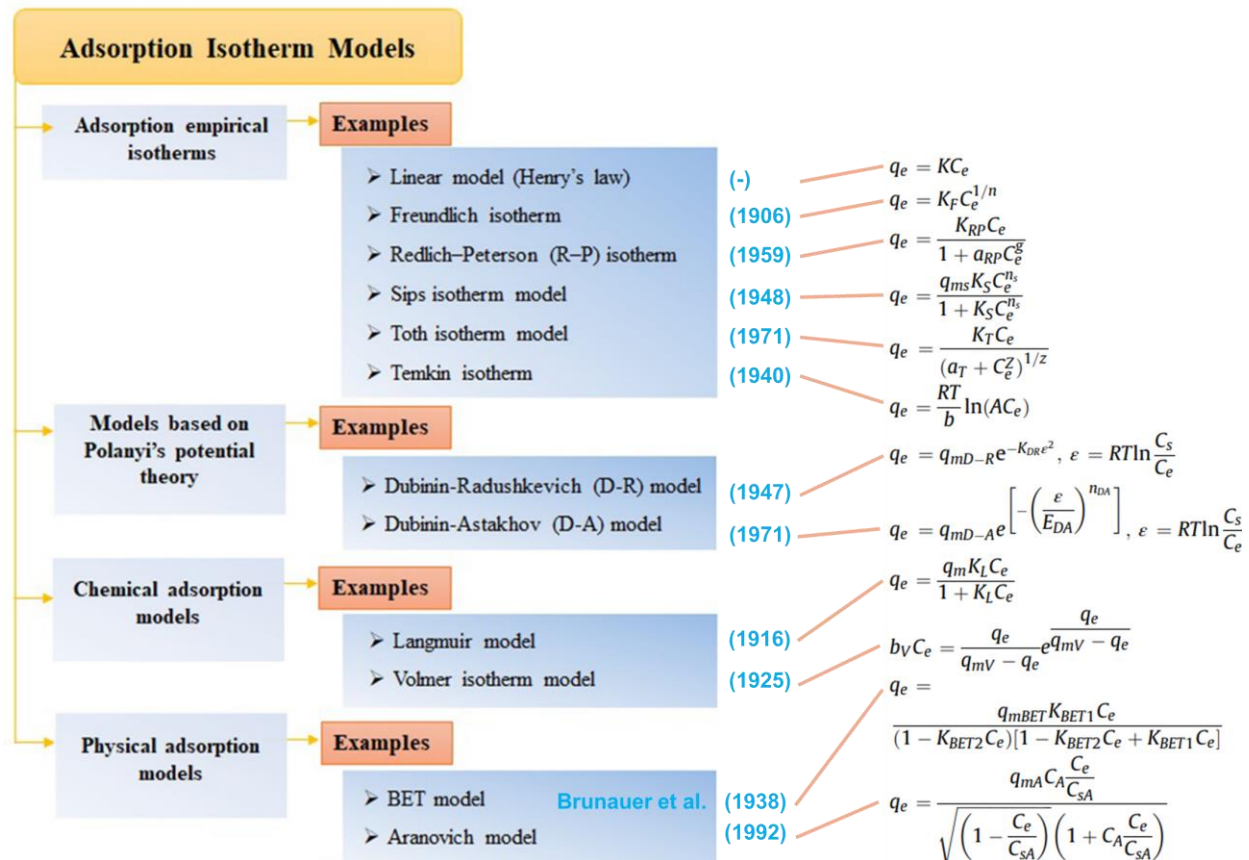


Figure 18 Classification, reference and equation of adsorption isotherm models
(Saleh, 2022; Wang & Guo, 2020)

2.4 Fixed-bed BTC models

2.4.1 Pore and Surface Diffusion Model (PSDM)

The pore and surface diffusion model (PSDM) is a very complete diffusion-based model (Xu et al., 2013). It is also called a 'general rate' model and classified as mass transfer model. Namely, this model is able to describe mass transfer very well and assumes that the adsorption reaction is instant. It is true that in porous materials like GAC, the adsorption of micropollutants is typically rate-limited by the intraparticle diffusion step and not by the adsorption reaction step. The fact that the PSDM includes a combination of all mass transfer resistances: external, fluid film, pore (macropore) and surface (micropore) diffusion, makes the model very interesting for adsorption of various micropollutants onto GAC (Inglezakis et al., 2019). From the earlier discussed four possibly rate-limiting steps in an adsorption column, the ones that are included in the model are marked green. It is called a multi-phase model because it takes into account multiple types of diffusion: film, pore and surface diffusion (S. Sharma et al., 2023).

- (1) Liquid phase mass transfer
- (2) External film diffusion
- (3) Intraparticle diffusion: Pore diffusion and Surface diffusion
The isotherm
- (4) The adsorption- desorption reaction

(1) Liquid phase mass transfer. Solutes can move through the column in axial or radial direction. However, as the length of the column is typically larger and radial velocities are rather small, only axial movement can be considered. It is then assumed that the cross-sections are homogeneous. A macroscopic mass conservation equation is required to include variations in the column in z-direction. These variations are: concentration of adsorbed adsorbate q , concentration of the bulk solution C , distance to inlet z , superficial velocity u and axial dispersion coefficient D_z (Xu et al., 2013). The variations are included in the differential mass balance equation (5).

$$\varepsilon_b \frac{\partial C}{\partial t} + u \frac{\partial C}{\partial z} + (1 - \varepsilon_b) \rho_b \frac{\partial q}{\partial t} = D_z \frac{\partial^2 C}{\partial z^2} \quad (5)$$

In which (Jarvie et al., 2005):

- ε_b = bed porosity or bed void fraction (-)
- ρ_b = bed (adsorbent) density (g/cm^3)

Mostly, axial dispersion is ignored so the right-hand side of the equation becomes zero. Mass conservation in the column with the components of the differential mass balance equation is shown in **Figure 19**. Mass balances are necessary to simulate the movement of the mass transfer zone as seen in **Figure 15**. The mass balance equation is generally applied in fixed-bed BTC models (Xu et al., 2013).

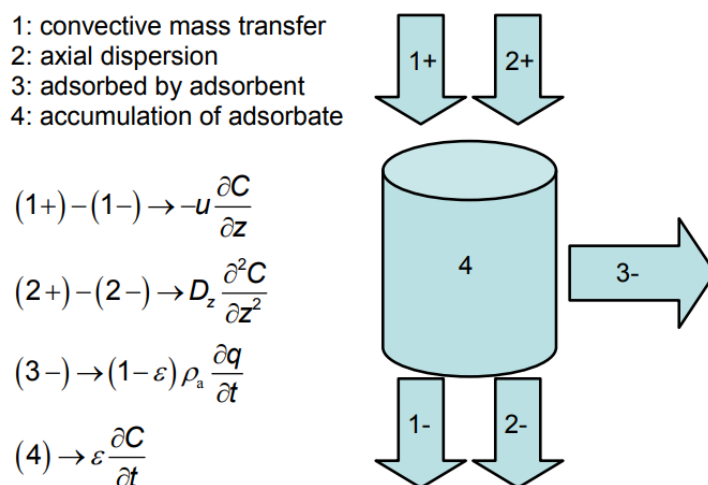


Figure 19 Schematic representation of mass conservation in the column with components of the differential mass balance equation (Xu et al., 2013)

Assumptions of this mass balance equation are: the packing material is made of spherical and uniform porous particles, the bed is homogenous and the concentration gradient in the radial direction of the bed is negligible, the flow rate is constant and does not vary within the column (Xu et al., 2013).

The PSDM simulates mass transfer in the bulk liquid via the liquid diffusivity coefficient D_l (cm^2/s), which is compound-specific. This parameter can be estimated from equation (6). V_b (cm^3/mol) is the molar volume of the synthetic organic compound (SOC) at the boiling point temperature and μ_l (centipoise) the liquid viscosity (Jarvie et al., 2005).

$$D_l = \frac{13.26 * 10^{-5}}{\mu_l^{1.14} V_b^{0.589}} \quad (6)$$

(2) External film diffusion is also included in the PSDM model. External film diffusion occurs within the film surrounded by every particle, also called the ‘boundary layer’. This layer is located at the interface between the exterior surface of the adsorbent particle, and the bulk solution. In some cases, film diffusion can predominate and thus be the rate-controlling step within the general rate model. At the adsorbent surface, the solute-/ sorbent concentrations are assumed to be in equilibrium. In the bulk liquid, concentration of pollutants are higher. Thus, the driving force for film diffusion is the concentration gradient (Xu et al., 2013). External diffusion is covered by equation: (7), (Worch, 2008).

$$\frac{dq}{dt} = \frac{k_F a_V}{\rho_b} (C - C_s) \quad (7)$$

Where

$$a_V = \frac{3}{r_p} (1 - \varepsilon_b) \quad (8)$$

- $k_F a_V$ = volumetric film diffusion mass transfer coefficient (1/s)
- ρ_b = bed density (g/cm³)
- C = concentration in the bulk liquid (mg_{solute}/L)
- C_s = concentration at the external particle surface (mg_{solute}/L)
- a_V = area available for mass transfer per reactor volume (cm²/cm³)
- r_p = radius adsorbent particle (cm)

k_F (cm/s) is the external mass transfer coefficient and can be estimated from the correlation of Gnielinski, 1978. This can be seen in equation (9), (Jarvie et al., 2005). It is clear that k_F depends on the adsorbent particle and liquid properties.

$$k_f = \frac{(1 + 1.5(1 - \varepsilon_b))\phi D_l}{2r_p} [2 + 0.644Re^{1/2}Sc^{1/3}] \quad (9)$$

The parameters Re and Sc from this correlation are then estimated by equations (10) and (11) (Jarvie et al., 2005)

$$Re = \frac{2\rho_l r_p V}{\varepsilon_b \mu_l} \quad (10)$$

$$Sc = \frac{\mu_l}{\rho_l D_l} \quad (11)$$

In which

- ϕ = adsorbent particle shape correction factor (-)
- Re = Reynolds number (-)
- Sc = Schmidt number (-)
- ρ_l = density of the water (g/cm³)
- V = superficial loading velocity (cm/s)

(3) Intraparticle diffusion is well-covered by the PSDM as it both includes surface and pore diffusion, which are represented by the intraparticle mass transfer coefficients, respectively D_s and D_p . These parameters can be estimated from the correlations of Crittenden, 1987 (equation (12)) and Zimmer, 1988 (equation (13)). These are equations from the ‘fixed-bed model parameter estimation’ review by (Jarvie et al., 2005).

$$D_s = SPDFR * \left[\frac{D_l \varepsilon_p C_0}{\tau_p K C_0^{1/n} \rho_a} \right] \quad (12)$$

$$D_p = \frac{D_l}{\tau_p} \quad (13)$$

- $SPDFR$ = surface to pore diffusion ratio (-)
- ε_p = adsorbent particle void fraction (-)
- C_0 = average influent liquid-phase concentration ($\mu\text{mole/L}$)
- τ_p = tortuosity of diffusion path length within particle (-)
- ρ_a = Apparent adsorbent particle density (g/cm^3)
- D_s = surface diffusion coefficient (cm^2/s)
- D_p = pore diffusion coefficient (cm^2/s)

Because both pore and surface diffusions are considered, the model is called heterogeneous. The mathematical differential equation to be numerically solved is given by equation (14) (S. Sharma et al., 2023). The mass transfer uptake rate in the GAC granule is described using Fick’s law (Xu et al., 2013).

$$\frac{\partial q}{\partial t} = D_s \left(\frac{\partial^2 q}{\partial r^2} + \frac{2}{r} \frac{\partial q}{\partial r} \right) + \frac{D_p}{\rho_p} \left(\frac{\partial^2 C_p}{\partial r^2} + \frac{2}{r} \frac{\partial C_p}{\partial r} \right) \quad (14)$$

The uptake rate $\frac{\partial q}{\partial t}$ both depends on surface and pore diffusion. r (cm) is the radial coordinate and is zero at the centre of the adsorbent particle. Thus, the deeper in the pores of the particle, the higher the uptake rate. ρ_p is the adsorbent particle density (g/cm^3) and C_p the concentration inside the pores ($\mu\text{g/L}$).

Locally, the fluid phase concentration at the adsorbent particle surface C_s is related to the adsorption capacity at the particle surface q_s by the equilibrium relationship, equation (15), which is often the Freundlich isotherm (Inglezakis et al., 2019).

$$q_s = f(C_s) \quad (15)$$

As said before, the adsorption reaction is not rate-limiting but assumed to be instant. An overview of the partial differential equations used in the PSDM model is seen in **Figure 20**. On the left-hand side, the external mass transfer in the fluid film is illustrated, with the concentration gradient being the linear driving force. Equations are similar but in the form of mass flux instead of uptake rate. Once at the adsorbent surface, equilibrium is obtained. Here, the Freundlich single-solute isotherm is used to calculate the amount of mass adsorbed q ($\text{mg}_{\text{solute}}/\text{g}_{\text{carbon}}$). The solute can also first diffuse inside the particle with a mass flux shown at the right-hand side of the figure. Diffusion mechanisms are simplified using two diffusion coefficients for pore and surface (Jarvie et al., 2005; S. Sharma et al., 2023).

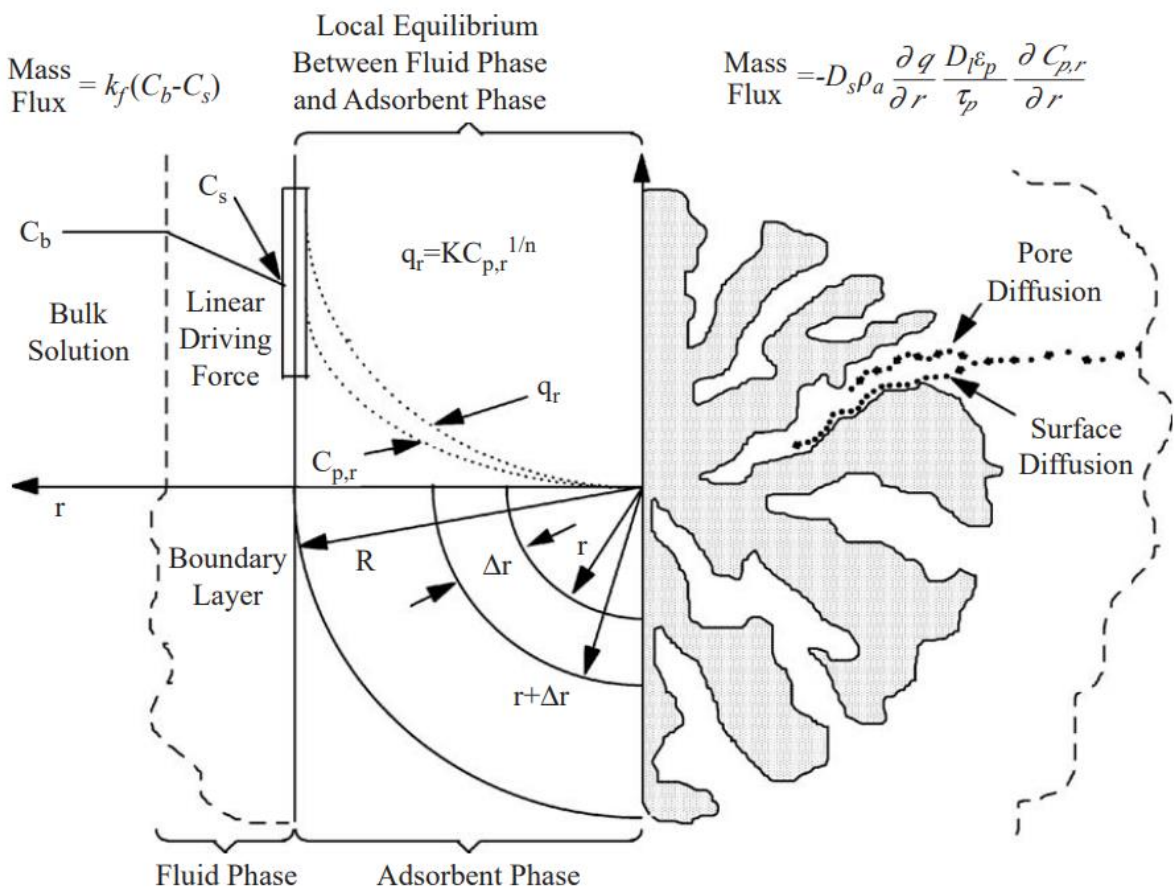


Figure 20 Schematic overview of the pore surface diffusion model (PSDM) and the mechanisms that are included in its partial differential equations (Jarvie et al., 2005)

2.4.2 Homogeneous Surface Diffusion Model (HSDM)

The homogeneous surface diffusion model is also a diffusion-based, mass transfer model which assumes that surface diffusion is predominant and pore diffusion is negligible, meaning a homogeneous adsorbent particle. This 'general rate' model is originally based on Fick's law with the PSDM being an extension of it. HSDM is a more simple and popular model, with a simplified differential equation (16) for the uptake rate which is related to the surface diffusion. Equation (7) is still valid for external film diffusion and the equilibrium relationship involves the same calculation by equation (15) (Inglezakis et al., 2019). The steps related to fixed-bed adsorption that are included in the HSDM are marked green. It is called a two-phase model as it considers two diffusion types: intraparticle surface and external film diffusion (S. Sharma et al., 2023).

- (1) Liquid phase mass transfer
- (2) External film diffusion
- (3) Intraparticle diffusion: Pore diffusion and Surface diffusion
The isotherm
- (4) The adsorption- desorption reaction

$$\frac{\partial q}{\partial t} = D_s \left(\frac{\partial^2 q}{\partial r^2} + \frac{2}{r} \frac{\partial q}{\partial r} \right) \quad (16)$$

2.4.3 Pore Diffusion Model (PDM)

The pore diffusion model is also a variant of the complete PSDM which assumes that pore diffusion is predominant and surface diffusion is negligible. It is less common than the HSDM but it is represented by partial differential equation (17). From the four possibly rate-limiting steps in an adsorption column, the ones that are included in the model are marked green. Mass balance and diffusion equations are again similar as in the prior described PSDM, except for surface diffusion. It is called a two-phase model as it considers two diffusion types: intraparticle pore and external film diffusion (S. Sharma et al., 2023).

- (1) Liquid phase mass transfer
- (2) External film diffusion
- (3) Intraparticle diffusion: Pore diffusion and Surface diffusion
The isotherm
- (4) The adsorption- desorption reaction

$$\frac{\partial q}{\partial t} = \frac{D_P}{\rho_P} \left(\frac{\partial^2 C_P}{\partial r^2} + \frac{2}{r} \frac{\partial C_P}{\partial r} \right) \quad (17)$$

2.4.4 Linear Driving Force (LDF) model

The linear driving force (LDF) model is a diffusion-based model and an approximation to the exact but much more complicated PSDM. The model is based on a simplified mass transfer equation(18) with an all-in-one or ‘lumped’ intraparticle mass transfer coefficient k (S. Sharma et al., 2023; Xu et al., 2013). It states that the rate of adsorption is proportional to the amount of adsorbate still required to achieve equilibrium, which is covered by the driving force factor ($q_s - q_a$). q_s is the equilibrium adsorption amount at the external particle surface and is related to C_s by an appropriate adsorption isotherm (equation (15)). q_a is the mean loading in the particle. The uptake rate $\frac{dq}{dt}$ depends on the linear difference between both. External diffusion can be considered by including equation (7) (S. Sharma et al., 2023; Worch, 2008). The steps included in the LDF model are marked green. It is called a two-phase model as it considers both intraparticle and external film diffusion (S. Sharma et al., 2023).

- (1) Liquid phase mass transfer
- (2) External film diffusion
- (3) Intraparticle diffusion: lumped mass transfer coefficient
The isotherm
- (4) The adsorption- desorption reaction

$$\frac{dq}{dt} = k(q_s - q_a) \quad (18)$$

A comparison of the PSDM model and LDF model is depicted in **Figure 21**. It can be seen that for the LDF model, an average q_a of the adsorption capacity is used for calculating the linear driving force and thus uptake rate. Namely, the solid pink line represents the average of the dashed pink line and increases over time. At each point in time, the sloped black arrow represents the linear difference ($q_s - q_a$). The uptake rate becomes smaller as the linear difference becomes smaller. In the end, there is no difference anymore (horizontal black arrow). In both cases, after some time the particle loading is maximized, i.e. equal to equilibrium loading, as the granule is fully saturated.

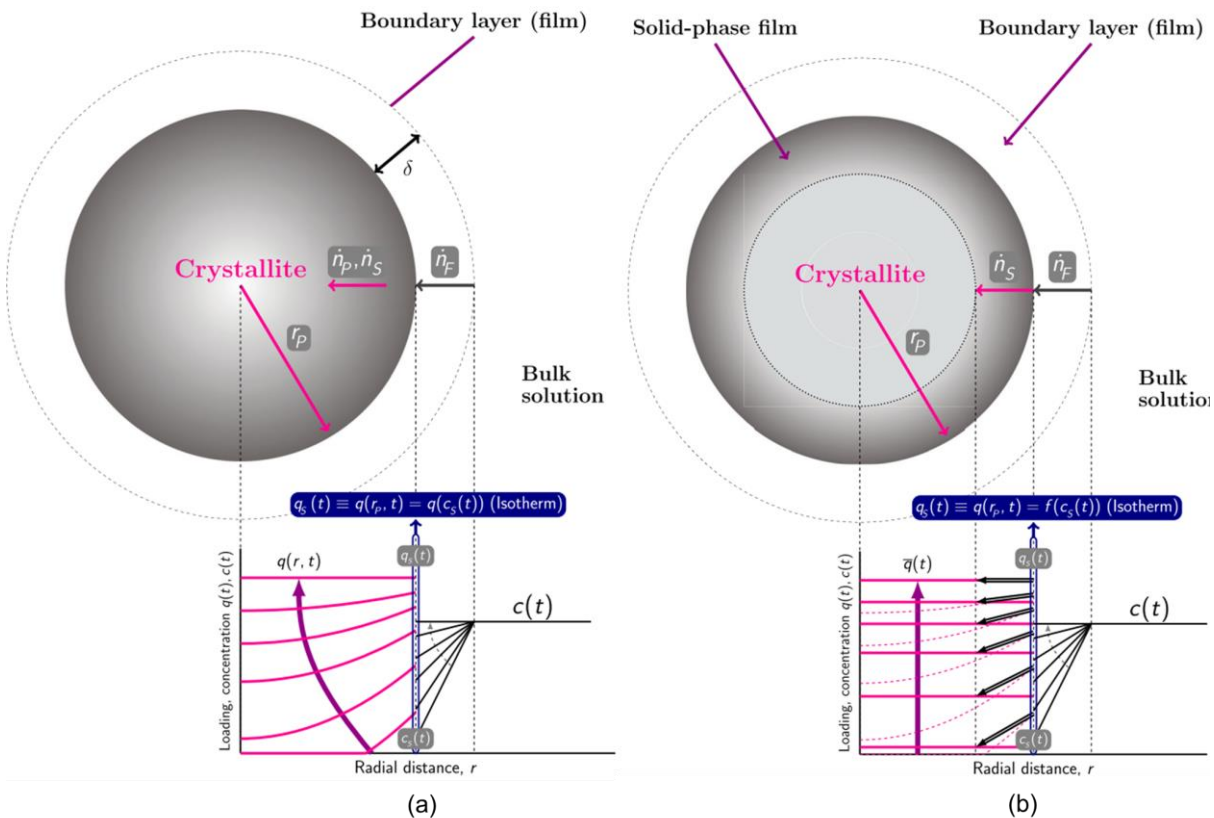


Figure 21 loading and concentration profiles of the (a) PSDM model with \dot{n}_p and \dot{n}_s respectively the flux by pore and surface diffusion, (b) LDF model with \dot{n}_s the solid flux driven by the linear driving force ($q_s - q_a$), black arrows. For both, \dot{n}_F is the film flux (i.e. external film diffusion) driven by the concentration gradient ($C - C_s$). The surface is considered to be in equilibrium and the adsorbent loading is calculated from the isotherm $q_s = f(c_s)$ (S. Sharma et al., 2023)

2.4.5 The Thomas model (TM) and Clark model (CM)

The Thomas and Clark models are only suitable where external and internal diffusion resistances are extremely small (Xu et al., 2013). These models neglect intraparticle diffusion and are also called ‘chemical kinetic models’. Mass transfer rate is assumed to be the difference between two opposing second-order reactions with different rate constants. It is assumed that there is local equilibrium in any cross-section along the bed. The Thomas model uses the Langmuir isotherm. The Clark model describes mass transfer in combination with the Freundlich isotherm. From the earlier discussed four possibly rate-limiting steps in an adsorption column, the ones that are included in the model are marked green. The Thomas and Clark model are examples of one-phase models because it takes into account only chemical kinetic mass transfer and the isotherm. Other one-phase models include the Bohart-Adams model and the Yoon-Nelson model (S. Sharma et al., 2023). The equations of these models can be found in the comprehensive review of fixed-bed column adsorption from (Patel, 2019).

- (1) Liquid phase mass transfer
- (2) External film diffusion
- (3) Intraparticle diffusion: Pore diffusion and Surface diffusion
The isotherm
- (4) **The adsorption- desorption reaction**

2.4.6 Pseudo-First-Order (PFO) model

The pseudo-first-order (PFO) model by Lagergren, 1898, is not diffusion-based but is an ‘adsorption reaction model’. It is only valid when the adsorption reaction itself (particularly chemisorption) is rate-limiting, without any concern about the diffusion mechanism. The model describes conditions where the number of active sites is significantly lower than the number of adsorbates (Wang & Guo, 2023). The focus is on the adsorption reaction near the active sites and diffusion or mass transfer is fast enough to be neglected (Silva et al., 2021). Moreover, the model does not include any isotherms (Inglezakis et al., 2019). The steps related to fixed-bed adsorption that are included in the PFO model are marked green. It is called a zero-phase model because the model ignores mass transfer and assumes instantaneous equilibrium (S. Sharma et al., 2023).

- (1) Liquid phase mass transfer
- (2) External film diffusion
- (3) Intraparticle diffusion
- The isotherm
- (4) **The adsorption reaction: chemisorption**

The mathematical description of the PFO model is seen in equation (19) (Wang & Guo, 2023).

$$\frac{dq_t}{dt} = k_1(q_e - q_t) \quad (19)$$

In which:

- q_t = adsorption capacity at time t (mg_{solute}/g_{carbon})
- q_e = equilibrium adsorption capacity (mg_{solute}/g_{carbon})
- k_1 = PFO rate constant (1/h)

k_1 is then the reaction rate constant with chemical reaction being the controlling step. The PFO model has the same form as the LDF model but it is not diffusion-based and no isotherm is included. Lagergren’s model is criticized in numerous papers for being theoretically inconsistent. However, it is mentioned here because, just as the PSO model, it has been extensively used in literature. It is a highly simplified empirical equation with absence of physical significance if underlying assumptions are not observed. The flexible mathematical formula is a descriptive tool rather than a predictive tool (Inglezakis et al., 2019). Therefore, The reaction-based models are not considered for higher scale predictions.

2.4.7 Pseudo-Second-Order (PSO) model

Next to the PFO model, the pseudo-second-order (PSO) kinetics model is also popular due to its simplicity. The model describes conditions where the number of active sites has the same order of magnitude as the number of adsorbates (Wang & Guo, 2023). Theoretically, PSO assumes that the rate-limiting step is most likely the chemical, strong covalent bonding, so again chemisorption (Inglezakis et al., 2019). It is together with the PFO categorized under the group of reaction kinetics-based models (Inglezakis et al., 2019). The mathematical description of the PSO is seen in equation (20) or integrated in equation (21). Plotting $\frac{t}{q_t}$ against time (equation (22)) at different activated carbon quantities can be used to estimate the second-order-rate constant of sorption k_2 (Aliakbarian et al., 2015). The steps related to fixed-bed adsorption that are included in the PSO model are marked green.

It is called a zero-phase model because the model ignores mass transfer and assumes instantaneous equilibrium (S. Sharma et al., 2023).

- (1) Liquid phase mass transfer
- (2) External film diffusion
- (3) Intraparticle diffusion
- The isotherm
- (4) **The adsorption reaction: chemisorption**

$$\frac{dq_t}{dt} = k_2(q_e - q_t)^2 \quad (20)$$

$$q_t = \frac{q_e^2 k_2 t}{1 + q_e k_2 t} \quad (21)$$

$$\frac{t}{q_t} = \frac{1}{k_2 q_e^2} + \frac{t}{q_e} \quad (22)$$

In which:

- q_t = adsorption capacity at time t (mg_{solute}/g_{carbon})
- q_e = equilibrium adsorption capacity (mg_{solute}/g_{carbon})
- k_2 = PSO rate constant (g/(h^{*}mg))

Being a purely empirical fitting exercise lacking physical significance, this model is also not ideal in varying conditions. This makes it unreliable for modelling urban wastewater treatment. Unfortunately, many researchers evaluated the applicability only on the quality of the fit on the experimental data and not on underlying theory, which is clearly a misperception (Inglezakis et al., 2019; Yao & Zhu, 2021).

2.5 Conclusion BTC models

An overview of the discussed BTC models with classification is given in **Table 5**. Zero-phase models such as the PFO or PSO model lack physical significance, are empirical and therefore more suitable as descriptive tool. One-phase models such as the Thomas or Clark model consider chemical mass transfer but neglect intraparticle diffusion. This is a drawback because in porous materials like GAC, the adsorption of micropollutants is typically rate-limited by intraparticle diffusion (Inglezakis et al., 2019). Two-phase models are then a better approximation and more accurate than one-phase models, but from here numerical solvers are required. Some intraparticle and external diffusion is considered. The HSDM, PDM and LDF are therefore realistic candidates for modelling the removal of micropollutants to some extent. Multi-phase models like the PSDM model are very complex but this complexity can be worth including when modelling adsorption of variable-size micropollutants under the highly varied conditions present in municipal wastewater. With detailed simulation of intraparticle diffusion (pore and surface), the PSDM is a strong candidate for simulating GAC in wastewater treatment plants. It is still worth mentioning that dynamic adsorption is a very complicated process and even multi-phase models are still simplified from reality: fast adsorption reaction rate, adsorbent granules of equal size in the column, no wall effect... Also, as said more effort is needed to determine the model parameters and numerical solvers are required (S. Sharma et al., 2023; Xu et al., 2013).

Table 5 Classification of fixed-bed adsorption models according to complexity (S. Sharma et al., 2023)

| <i>Fixed-bed model</i> | Zero-phase | One-phase | Two-phase | Multi-phase |
|------------------------|---|---|---|--|
| <i>Description</i> | Ignores mass transfer and assumes instantaneous equilibrium | Include isotherm but neglect intra-particle diffusion. Not very accurate in describing breakthrough behaviour in a column | Take into account both film and intraparticle diffusion. More accurate than one-phase but have to be solved numerically | Take multiple types of diffusion into account: film diffusion, pore diffusion and surface diffusion. However, surface reaction rates assumed to be much faster than diffusion, thus adsorption rate not controlling step |
| PSDM | | | | ✗ |
| HSDM | | | ✗ | |
| PDM | | | ✗ | |
| LDF | | | ✗ | |
| Thomas model | | ✗ | | |
| Clark model | | ✗ | | |
| PFO | ✗ | | | |
| PSO | ✗ | | | |

MATERIALS AND METHODS

The tool that is used for simulation of GAC adsorption is the PSDM model implemented in Python by USEPA. Additional plots, edits of the PSDM USEPA code and extensions can be found in the GitHub of this thesis, where folders are organized according to the chapters and structure of thesis text:

<https://github.com/matcoghe/Thesis-Modelling-activated-carbon.git>

- 6.1 Isotherm fitting tool
- 6.2 Example modelling of compound TCE
- 6.3 Pilot modelling of compound PFHpA
- 6.4 USEPA fouling approach
- 7.1 Extending the USEPA fouling approach
- 7.2 Alternative fouling approach
- 7.3 Uncertainty analysis of Freundlich parameters

The PSDM model was executed from a *notebook* (*.ipynb*), that also shares the name of the respective section in this document. The notebook uses the scripts PSMD.py, PSDM_extra.py, PSDM_functions.py and PSDM_tools.py. Edits or extensions are highlighted with //Mathieu (Ctrl+F).

Language and grammar of the thesis text is optimized with help of ChatGPT. Paragraphs were written by the author, only sentences or words were adjusted through advice of AI.

3 USEPA PSDM MODEL

The United States Environmental Protection Agency (USEPA) implemented the Pore and Surface Diffusion Model (PSDM) into Python and made it available as open-source code on GitHub https://github.com/USEPA/Water_Treatment_Models/tree/master/PSDM (J. Burkhardt, 2020). The model was derived from an earlier AdDesignS™ version from Michigan Technological University. These software packages were originally developed for cleaning up contamination sites all over the United States. The objective was to estimate how effective adsorption was in the removal of fuel from contaminated water that was coming from leaking storage tanks in California (Hokanson et al., 1999).

As explained in Chapter 2, the PSDM is a good candidate BTC model for simulating the adsorption of micropollutants by GAC in full-scale systems. The diffusion-based, multi-phase model describes intraparticle diffusion very well, at both pore and surface level. This is necessary as intraparticle diffusion is typically rate-limiting for porous materials like GAC, and very variable (Inglezakis et al., 2019). This can be seen in **Figure 14**, where the diffusion type depends on the size of the pollutant and diameter of the pores. There is an automated parameter-fitting and parameter-estimation tool included in the EPA model. Further, it is possible to consider the fouling phenomenon, i.e. competition of dissolved organic carbon (DOC) with micropollutants for the adsorption sites. Fouling is often also referred to as preloading by natural organic matter (NOM) (J. Burkhardt et al., 2022).

To understand how the PSDM model works, one can refer to **paragraph 2.4.1**, where the equations are presented in the sequence of steps that the solute undergoes in a fixed-bed column. A summarizing overview of the PSDM mechanisms for one GAC granule is seen in **Figure 20**. These granules are assumed to have the same size and be equally distributed in the column. Equations are shown next to the equations of the USEPA model in **Table 6**.

Relevant model parameters of the USEPA PSDM model are listed in **Table 7**. It can be noticed that the bed has two dimensions; length and diameter. Thus, the PSDM model by EPA assumes a cylindrical fixed-bed column. The apparent particle density (ρ_a) is the mass of the AC granule (particle) divided by the apparent (solid) particle volume (Webb, 2001). Tortuosity of the particle (τ_p) is the ratio of the actual diffusion path length (L_e) to the shortest, straight path length (L) of a flow in the GAC particle (Mudhoo et al., 2024). Partial differential equations are solved with the orthogonal collocation numerical solver (J. Burkhardt et al., 2022). The number of radial and axial collocation points represent the number of nodes in the radial and axial direction in the column respectively. The problem is simplified to a 2D problem. For every node location, concentrations are calculated using the partial differential equations. Axial collocation points are usually the most significant in a long cylinder. Model correlations (23) and (24) are used to calculate bed porosity (ε_b) and empty bed contact time ($EBCT$) (J. Burkhardt, 2020).

$$\varepsilon_b = 1 - \frac{\text{Weight bed (wt)}}{\text{Volume bed} * \text{Particle density} (\rho_p)} \quad (23)$$

$$EBCT = \frac{\text{Area} * L (= \text{volume column})}{\text{Flow rate} (flrt)} \quad (24)$$

Table 6 Model equations of the PSDM model by USEPA in Python language

| Mathematical equations (Jarvie et al., 2005) | Equations USEPA code (J. Burkhardt, 2020) |
|--|--|
| Mass balance differential equation | |
| $\varepsilon_b \frac{\partial C}{\partial t} + u \frac{\partial C}{\partial z} + (1 - \varepsilon_b)\rho_b \frac{\partial q}{\partial t} = D_z \frac{\partial^2 C}{\partial z^2}$ | Mass balance |
| Uptake rate differential equations | |
| $\frac{dq}{dt} = \frac{k_F a_V}{\rho_b} (C - C_s)$ | External film |
| $\frac{\partial q}{\partial t} = D_s \left(\frac{\partial^2 q}{\partial r^2} + \frac{2}{r} \frac{\partial q}{\partial r} \right) + \frac{D_p}{\rho_p} \left(\frac{\partial^2 C_p}{\partial r^2} + \frac{2}{r} \frac{\partial C_p}{\partial r} \right)$ | Granule |
| Isotherm equation (Freundlich) | |
| $q_e = K_F * C_e^{1/n}$ | <code>def freundlich(c, k, invN): return k * c**invN</code> |
| Parameter estimation equations | |
| $D_l = \frac{13.26 * 10^{-5}}{\mu_l^{1.14} V_b^{0.589}}$ | <code>difl = 13.26e-5/(((vw * 100.)**1.14)*(mol_vol**0.589))</code> |
| $k_f = \frac{(1 + 1.5(1 - \varepsilon_b))\phi D_l}{2r_p} [2 + 0.644 Re^{1/2} Sc^{1/3}]$ | <code>kf_v = multi_p*(1.+1.5*(1-ebed))*(2.+0.644*(re**0.5)*(sc**(1./3.)))</code> |
| $D_s = SPDFR * \left[\frac{D_l \varepsilon_p C_0}{\tau_p K C_0^{1/n} \rho_a} \right]$ | <code>ds_v = epor*difl*cb0*psdfr/(1e3*rhop*molar_k*cb0**xn_v)</code> |
| $D_p = \frac{D_l}{\tau_p}$ | <code>dp_v = (difl/(tortu))</code> |

Table 7 Model parameters of the PSDM model by USEPA: input, state and output parameters (J. Burkhardt, 2020)

| Parameter | | Model name | Unit | Type |
|----------------------------|--|------------|---|------------------|
| Input parameters | | | | |
| <i>Compound properties</i> | Molecular weight (MW) | mw | g/mol | fixed |
| | Molar volume (V_b) | mol_vol | ml/mol | fixed |
| | Boiling point (BP) | temp | °C | fixed |
| | Density compound | / | g/ml | fixed |
| <i>Isotherm parameters</i> | Freundlich parameter (K) | k | [$(\mu\text{g/g})(\text{L}/\mu\text{g})^{1/n}$] | fix (no fouling) |
| | Freundlich exponent ($1/n$) | xn | (-) | fixed |
| <i>Bed properties</i> | Radius particle (r_p) | rad | cm | fixed |
| | Porosity particle (ε_p) | epor | (-) | fixed |
| | Pore to surface diffusion ratio (<i>SPDFR</i>) | psdfr | (-) | fixed |
| | Particle density (ρ_p) | rhop | g/ml | fixed |
| | Apparent particle density (ρ_a) | rhof | g/ml | fixed |
| | Length bed | L | cm | fixed |
| | Diameter bed | diam | cm | fixed |
| | Weight bed | wt | g | fixed |
| | Flow rate | flrt | µg/min | fixed |
| <i>Raw data</i> | Tortuosity particle (τ_p) | tortu | (-) | fixed |
| | Influent concentration c(t) | infl | µg/L | fixed/var |
| <i>Numerical solver</i> | Effluent concentration c(t) | effl | µg/L | fixed/var |
| | Radial collocation points | nr | amount | fixed |
| | Axial collocation points | nz | amount | fixed |
| State variables | | | | |
| <i>State variables</i> | Concentration (t,x) | c | µg/L | variable |
| Output parameters | | | | |
| <i>Calculated output</i> | Effluent concentration c(t) | c | µg/L | variable |
| | Liquid diffusion coefficient (D_l) | difl | cm ² /s | fixed |
| | Film mass transfer parameter (k_f) | kf_v | cm/s | fixed |
| | Surface diffusion coefficient (D_s) | ds_v | cm ² /s | fixed |
| | Pore diffusion coefficient (D_p) | dp_v | cm ² /s | fixed |
| | Viscosity of water (μ_l) | vw | g/(cm*s) | fixed |
| | Density of water (ρ_l) | dw | g/cm ³ | fixed |
| | Bed porosity (ε_b) | ebed | (-) | fixed |
| | Empty bed contact time (EBCT) | ebct | (s) | fixed |

4 ARTICLE MODELLING PFAS REMOVAL USING GAC

The performance of GAC can be evaluated using modelling tools and the results support local decision makings to choose for it, if favourable. Burkhardt et al., 2022, evaluated the adsorption of 16 PFAS compounds under different scenarios through modelling. The pore and surface diffusion model from USEPA (chapter 3) was therefore utilized. PFAS removal was applied at pilot scale so model parameters could be calibrated based on experimental data. A dataset with other conditions, i.e. winter

instead of summer, was created and used to validate the model as good as possible. The Freundlich isotherm was applied with Freundlich parameters K and $1/n$ (J. Burkhardt et al., 2022).

Table 8 Input parameters for modelling the adsorption of PFHpA and TCE (J. Burkhardt et al., 2022)

| Parameter (J. Burkhardt, 2020) | | PFHpA | TCE | Unit | |
|--------------------------------|---|--|---|---|------|
| <i>Compound properties</i> | Molecular weight (MW) | 364.06 | 131.39 | g/mol | |
| | Molar volume (V_b) | 203.158 | 102 | ml/mol | |
| | Boiling point (BP) | 175 | 87 | °C | |
| | Density compound | 1.792 | 1.53 | g/ml | |
| <i>Isotherm parameters</i> | Freundlich parameter (K) | 6.764 | 5026.04 | $[(\mu\text{g/g})(\text{L}/\mu\text{g})^{1/n}]$ | |
| | Freundlich exponent ($1/n$) | 0.6 | 0.43 | (-) | |
| <i>Bed properties</i> | Radius particle (r_p) | 0.0513 | 0.0513 | cm | |
| | Porosity particle (ε_p) | 0.641 | 0.641 | (-) | |
| | Pore to surface diffusion ratio (SPDFR) | 5 | 5 | (-) | |
| | Particle density (ρ_P) | 0.803 | 0.803 | g/ml | |
| | Apparent particle density (ρ_a) | 0.62 | 0.62 | g/ml | |
| | Length bed | 120 | 276.5 | cm | |
| | Diameter bed | 10 | 304.8 (10 ft) | cm | |
| | Weight bed | 4349.95 (4.35 kg) | 9e6 (20000 lb) | g | |
| | Flow rate | 984.21 | 2146200 | g/min | |
| | Tortuosity particle (τ_p) | 1 | 1 | (-) | |
| <i>Raw data</i> | Influent concentration c(t) | day0 13 34 48 62 76 97 111 125 | 0.011 0.015 0.02 0.015 0.027 0.037 0.0426 0.0399 0.0509 | 50 000 | µg/L |
| | Effluent concentration c(t) | day0 13 34 48 62 76 97 111 125 | 0 0 0.0023 0.0046 0.011 0.02 0.0317 0.0366 0.0401 | / | µg/L |
| <i>Numerical solver</i> | Radial collocation points | 8 | 8 | amount | |
| | Axial collocation points | 11 | 12 | amount | |

One of the PFAS compounds under the loop for research was PFHpA. Its adsorption onto F400 GAC was studied in a pilot column with raw water influent coming from the Cape Fear River. Compound properties, bed properties and concentration values were derived from the article and listed in **Table 8**. Parameters that can not be derived from the article are taken from the 'TCE' example. This dataset was attached, as Excel sheet, to the GitHub repository of USEPA. Specifically, properties related to the GAC granules were not mentioned and thus assumed to be similar as the adsorption system TCE-F400.

The available dataset for the single solute PFHpA is interesting information since it can be used to test the open-source model. Moreover, the author of the Python code is the same as from the article; J. Burkhardt. All input parameters were fed to the PSDM model, which was done by filling in the input Excel sheet. It was an opportunity to test the model and check if the same breakthrough curve is obtained as in the PFAS article, see **Figure 22**. The simulation results served as a starting point for further research. Model mechanisms were better understood after investigation of the Python script. As the working became more clear, small extensions were made and some sensitivity was analysed of certain model parameters.

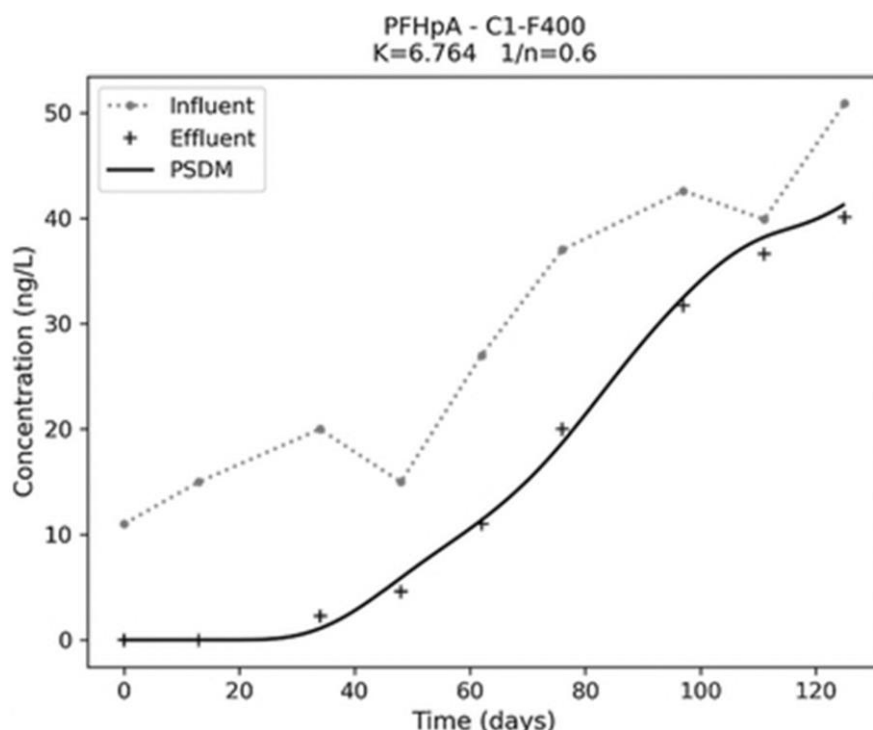


Figure 22 Influent and effluent data of micropollutant PFHpA in pilot adsorption column.
Solid line represents the PSDM model fit for the BTC (J. Burkhardt et al., 2022)

5 EUROPE INTERREG PROJECT AND AQUAFIN

Here tell my objectives in the context of the Aquafin project, these are extra simulations I can still do.

Proposal Mathieu:

- *use political-relevant compounds*
- *address their BTC and fouling (via alternative method so how much weight reduction + small sensitivity of isotherm parameters) for a column with dimensions of Aartselaar pilot plant*

RESULTS AND DISCUSSION

6 TESTING THE PSDM BY USEPA MODEL

In this chapter, mechanisms of the PSDM model by USEPA, see **Chapter 3**, were tested and investigated in Python. For this purpose, example data from the GitHub folders itself or experimental data from the PFAS article (J. Burkhardt et al., 2022), see **Chapter 4**, were utilized as input to feed the model. The implementation of the PSDM model into Python, that was used here, is open-source: https://github.com/USEPA/Water_Treatment_Models/tree/master/PSDM (J. Burkhardt, 2020).

6.1 Isotherm fitting tool

The PSDM model by USEPA (J. Burkhardt, 2020) includes a fitting tool for isotherm parameters in the '*Example_isotherm.py*' file. An example dataset consists of a list of datapoints (C_0 , C_e , mass). This dataset is normally derived from a lab experiment with a beaker, single-solute polluted water and activated carbon. An initial concentration (C_0) is added to a certain mass of carbon and after some time, equilibrium concentration (C_e) is measured. If the mass of carbon was zero, then $C_e = C_0$ because no adsorption took place. If a high mass of carbon was added to the batch experiment, the equilibrium concentration is typically low to zero because there was high adsorption capacity.

Based on the experimental dataset, the PSDM model automatically fits the desired isotherm. This is done by the *isotherm_fit* function in *PSDM_tools.py*. The function contains the isotherm equation of Freundlich, which is the default one, and makes use of the *curve_fit* from *scipy.optimize* for finding the right fit onto the dataset. This is an isotherm equation with two equilibrium parameters and is important for the model to later calculate adsorbed concentrations at the surface of the GAC, which is assumed to be in equilibrium. Datapoints, best fit by the isotherm model and estimated isotherm parameters are shown in **Figure 23**.

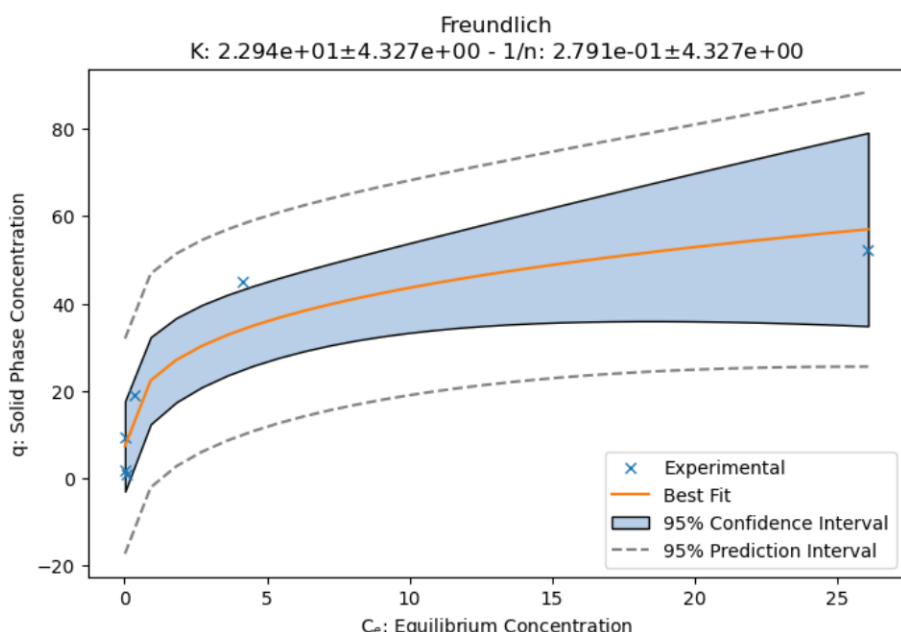


Figure 23 Isotherm fitting tool from USEPA (a) example dataset from batch equilibrium experiment (b) best fit Freundlich isotherm with equilibrium parameters K and 1/n

The `curve_fit` function from `scipy.optimize` was tested apart from the PSDM tools also. Its functioning was tested with a randomly generated but still realistic dataset. This dataset was formed based on the Freundlich isotherm ($K_F=2.7$, $n=3$) with some additional noise. The Python script was created with the help of ChatGPT and can be seen in **Figure 24**. The estimated isotherm curve fitted very well and Freundlich isotherm parameters were estimated, in a similar way as in the `PSDM_tools.py` script.

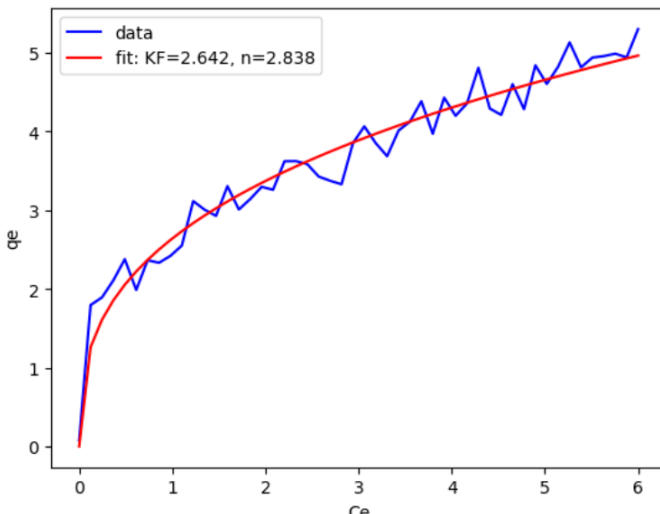


Figure 24 Isotherm fitting test with ‘`curve_fit`’ from ‘`scipy.optimize`’ (a) Python script
(b) Freundlich isotherm curve fit with estimated parameters

6.2 Example modelling of compound TCE

Executing the BTC model can be done from the notebook ‘`.ipynb`’. Example input data is found in *Example_TCE.xlsx*, where the input parameters from **Table 8 (TCE)** are classified under different sheets. The model estimates a breakthrough 27 days after fresh or regenerated GAC was added. The BTC, estimated by the USEPA PSDM model, is shown in **Figure 25**. The prediction is not linked to any experiment but is rather an example to show what the model output looks like.

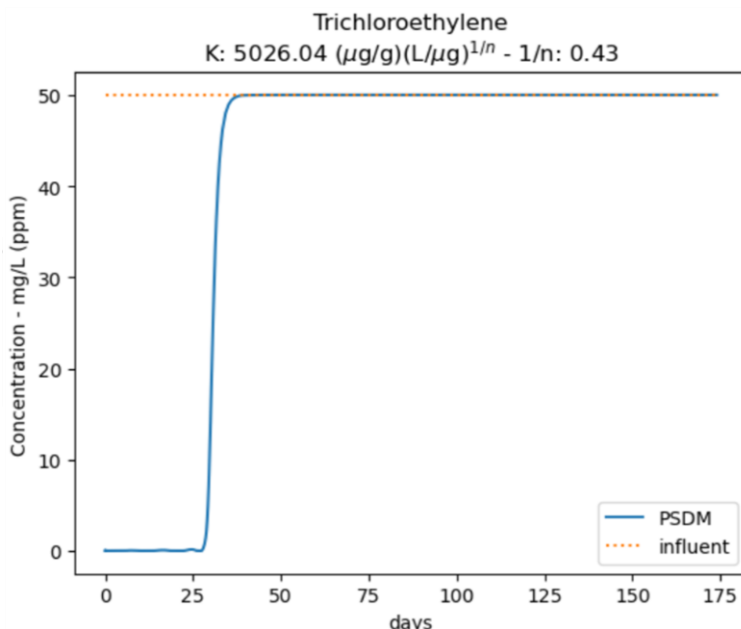


Figure 25 Example breakthrough prediction for the compound TCE
executed by the USEPA PSDM model (J. Burkhardt, 2020)

6.3 Pilot modelling of compound PFHpA

To test the PSDM model with a realistic study case, that is where the PFAS pilot study (**Chapter 4**) becomes interesting. Input parameters from **Table 8 (PFHpA)** were inserted under the different sheets in *Input_PFHpA.xlsx*. Fouling was also taken into account in the same way as in the research (J. Burkhardt et al., 2022). Specifically, *chem_type* was set to ‘PFAS’ and *water_type* to ‘Rhine’. The USEPA fouling approach will be later discussed.

6.3.1 Estimation of breakthrough curve

Figure 26 shows both the original model estimate and the replicated model estimate resulting from the USEPA Python code. To make the replication, the isotherm parameters K and 1/n, derived from the research, were given with the model input. On the contrary, the experimental effluent dataset was not given as input. The objective here was to get a free estimate of the effluent curve. Parameters that were not directly available in the paper were taken from the previous ‘TCE’ example, since also there the bed consists of F400 GAC. These were properties related to the GAC granules, which were not mentioned. It is not true that the model parameters were calibrated. They were derived from another study. However, this test demonstrated that the open-source model functioned very accurate and realistic, inspiring further investigation starting from this point of research.

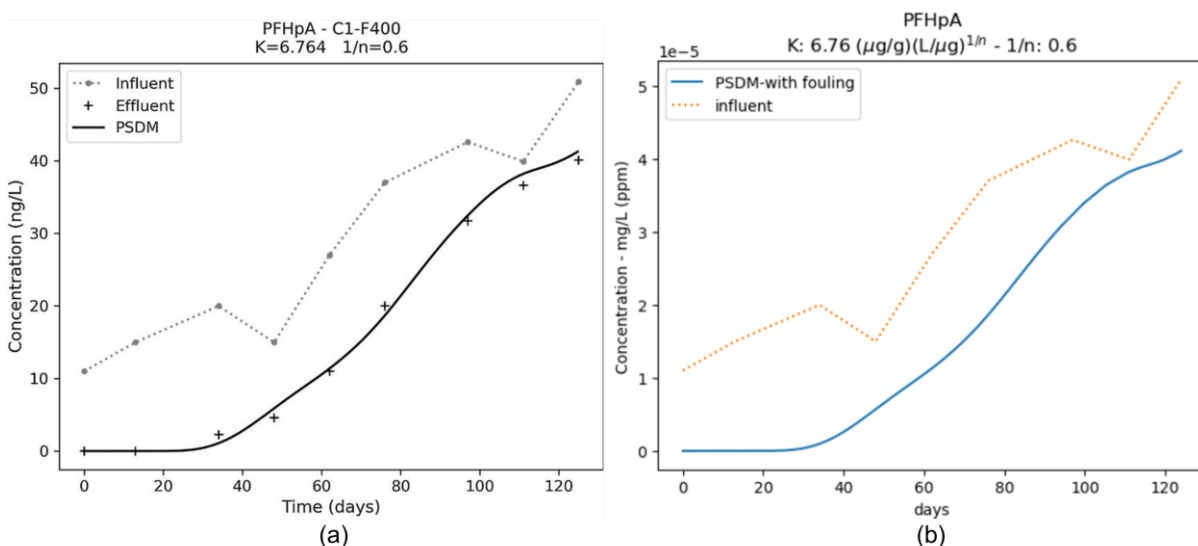
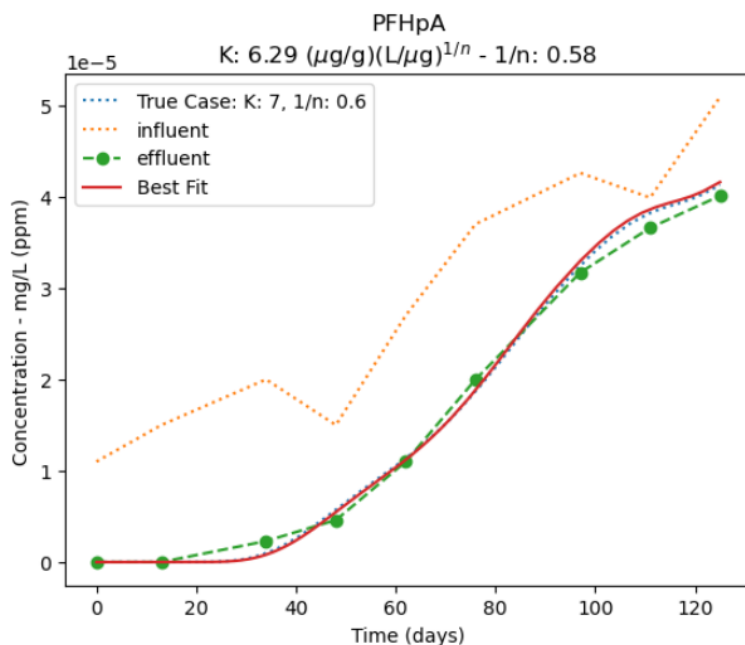


Figure 26 Breakthrough curve model prediction for fixed-bed adsorption of PFHpA: (a) prediction from scientific paper of Burkhardt et al., 2022, (b) replication in Python

6.3.2 Estimation of isotherm parameters

Originally, the purpose using the PSDM model in the case of **Figure 26(a)** was to estimate the Freundlich isotherm parameters K and 1/n through the automated fitting tool. To do so, experimental influent and effluent data was fed to the model by the researchers. For the thesis, the same tool was also applied by hiding isotherm parameters K and 1/n and introducing the effluent experimental dataset. Estimation of the isotherm parameters by the automated fitting tool can be seen in **Figure 27**. It can be concluded that, next to the BTC estimation, estimation of equilibrium parameters was also functioning very well. The predicted isotherm parameters were close to the ones estimated by the research paper. The red line is the best fit, which was found by 23x executing the *run_psdm_kfit* function. The amount was counted by defining a new parameter *psdm_teller* that counted the number of runs.



**Figure 27 Equilibrium parameters prediction by automated fitting tool of the PSDM model by USEPA.
(J. Burkhardt, 2020)**

6.4 USEPA fouling approach

There are many problems that can cause a lower capacity of the carbon, from which the effects of NOM have been found to be the most important (Magnuson & Speth, 2005):

- Competition for adsorption sites from other contaminants
- Competition from background natural organic matter (NOM)
- Preloading of NOM onto AC
- Other: T, pH, low MP concentration leading to desorption...

The USEPA fouling approach is based on the study of Magnuson & Speth, 2005, where preloading by NOM is mathematically described. GAC capacity is reducing over time due to an increase of preloading by NOM. Fresh carbon is initially not preloaded, but its capacity reduces as more NOM accumulates. As mentioned earlier in **section 2.3.1**, the Freundlich K_F is a constant for a given sorbate related to the sorption capacity. The idea of this fouling approach is thus to present a time dependent Freundlich K (K_t), as this parameter relates adsorption capacity for a certain sorbate. The reduction is empirically described in equation (25), where K_t is divided by K_0 for organic-free water (Magnuson & Speth, 2005).

$$\left(\frac{K_t}{K_0}\right)_{TCE} = 0.01 * [A1 - A2 * t + A3 * \exp(-A4 * t)] \quad (25)$$

This was empirically determined in a preloaded batch experiment for trichloroethylene at equilibrium. Fouling is simplified by assuming that the Freundlich K diminishes. To find $\left(\frac{K_t}{K_0}\right)$ for another solute, compound-specific correlation factors a and b need to be determined (Magnuson & Speth, 2005):

$$\left(\frac{K_t}{K_0}\right)_{contaminant} = a\left(\frac{K_t}{K_0}\right)_{TCE} + b \quad (26)$$

Because it is time-consuming to determine parameters a and b for all compounds, it is assumed the compound belongs to one of nine groups (see later). Determination of compound-specific parameters is done by use of quantitative structure-property relationships (QSPRs), equations (27) and (28).

$$a = -0.0624 \log K_{ow} - 1.15 \log \chi_2 - 0.166 N_{am} + 1.37 \quad (27)$$

$$b = 0.0441\alpha + 0.406D_{z(hybrid)} - 0.250 \quad (28)$$

Compound properties are (J. B. Burkhardt et al., 2022; Magnuson & Speth, 2005):

- K_{ow} = octanol-water partition coefficient
- χ_2 = second-order shape index
- N_{am} = sum of number of primary and secondary amine groups
- α = molecular polarizability
- $D_{z(hybrid)}$ = largest hybrid component of the dipole moment perpendicular to the long molecular axis

Also in other literature it is identified that BOM present in the water reduces the GAC capacity for SOCs. Jarvie et al., 2005, illustrated the reduction of the Freundlich capacity parameter K both experimentally and modelled by use of equation (25) for TCE (**Figure 28**).

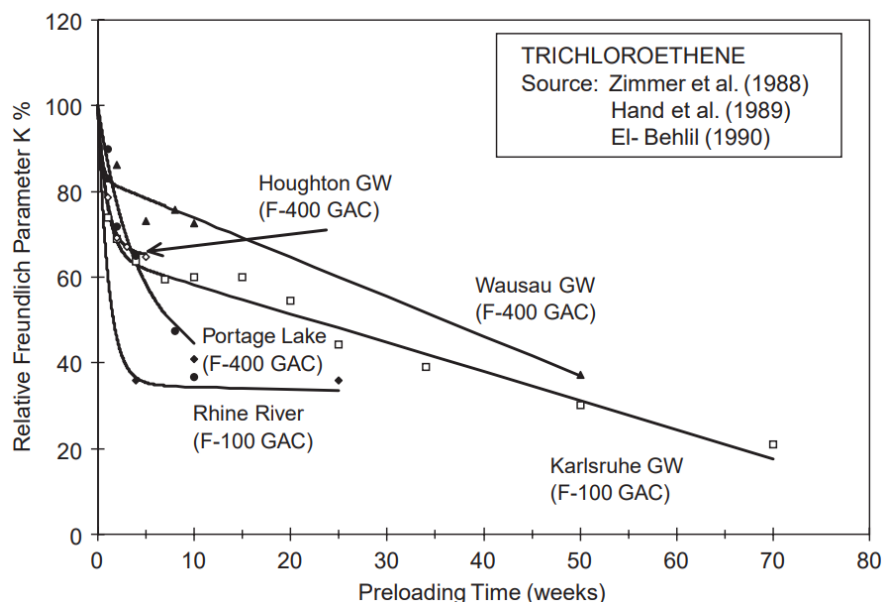


Figure 28 Reduction of Freundlich K for TCE and for various background waters (Jarvie et al., 2005)

In the PSDM by USEPA code (**Figure 29**), parameters $A1$, $A2$, $A3$ and $A4$ from equation (25) were presented as $rk1$, $rk2$, $rk3$ and $rk4$. These were calculated dependent on water-specific parameters $a1 - a4$ and compound-specific parameters $b1$ and $b2$, that represent a and b in equation (26). The fraction $(\frac{K_t}{K_0})_{contaminant}$ is defined as 'k_mult_pd'.

The fouling approach by USEPA was investigated by returning the fouling parameters during the pilot simulation of compound PFHpA (**paragraph 6.3**). Printed fouling parameters are shown for organic-free water and NOM preloaded river water in **Figure 30**.

```

a1, a2, a3, a4 = foul_params['water'][self.water_type]
b1, b2 = foul_params['chemical'][self.chem_type]
k_mult_pd = self.rk1_store[comp] + \
            self.rk2_store[comp] * t + \
            self.rk3_store[comp] * np.exp(self.rk4_store[comp] * t)
    rk1 = b1 * a1 + b2
    rk2 = b1 * a2
    rk3 = b1 * a3
    rk4 = b1 * a4

```

Figure 29 USEPA fouling approach: equations for Freundlich K reduction in Python (J. Burkhardt, 2020)

no fouling

```

a1: 1.0
a2: 0.0
a3: 0.0
a4: 0.0
b1: PFHpA 1.0
dtype: float64
b2: PFHpA 0.0
dtype: float64
rk1: PFHpA 1.0
dtype: float64
rk2: PFHpA 0.0
dtype: float64
rk3: PFHpA 0.0
dtype: float64
rk4: PFHpA 0.0
dtype: float64
//Mathieu: k_mult_pd: [1. 1. 1. 1. 1.] ...
a1: 0.35
a2: -6.15e-08
a3: 0.65
a4: -8.93e-05
b1: PFHpA 0.44
dtype: float64
b2: PFHpA 0.36
dtype: float64
rk1: PFHpA 0.514
dtype: float64
rk2: PFHpA -2.706000e-08
dtype: float64
rk3: PFHpA 0.286
dtype: float64
rk4: PFHpA -0.000039
dtype: float64
//Mathieu: k_mult_pd: [0.79595906 0.73885526] ...

```

fouling

Figure 30 USEPA fouling parameters for adsorption from 'organic-free' & 'Rhine' water.
Yellow = compound-specific fouling parameters for PFHpA

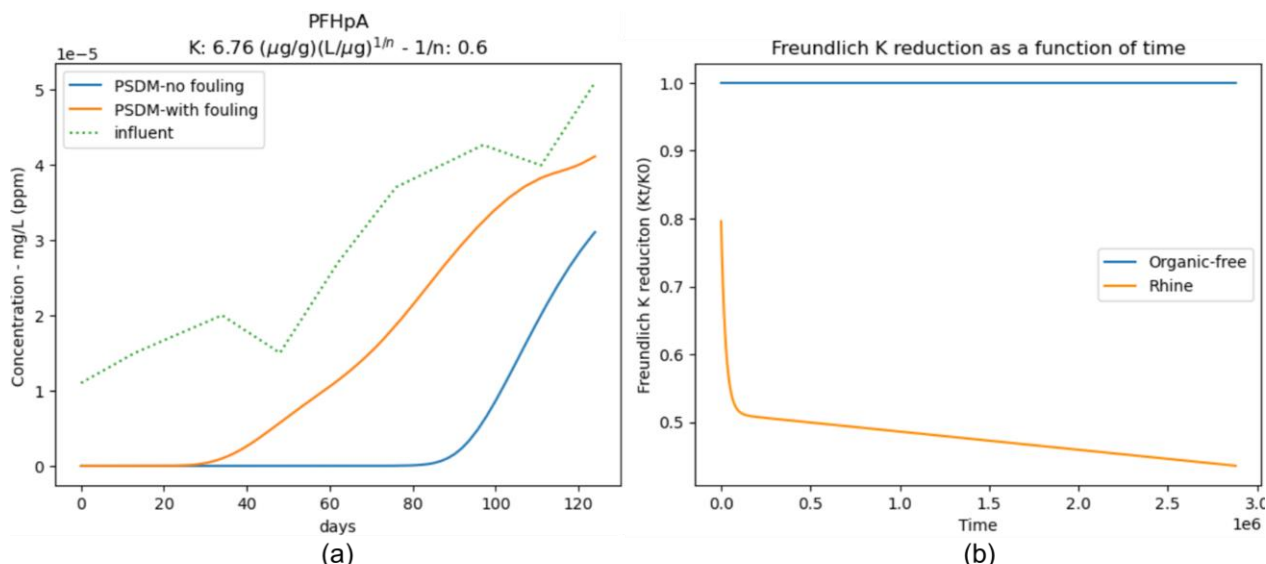


Figure 31 Comparison of fouling vs no fouling for fixed-bed adsorption of PFHpA:
(a) breakthrough curve model prediction, (b) Freundlich K reduction

It was obvious from **Figure 31(a)** that influence of fouling is indeed significant and so it is important to consider it during adsorption simulations. First breakthrough occurred almost 60 days earlier when considering fouling. **Figure 31(b)** confirms there is no Freundlich K reduction for organic-free water and clearly displays the orange declining curve. The reduced K ended up being more than half of the organic-free K. The function has a very similar shape as the 'Rhine River' function in **Figure 28**, where capacity reduction is fastest in the first weeks of simulation.

7 EXTENDING THE PSDM BY USEPA MODEL

In this chapter, small extensions and alternatives were added to the PSMD model by USEPA (J. Burkhardt, 2020). Model input data used here were again derived from the PFAS paper for PFHpA (J. B. Burkhardt et al., 2022) and from USEPA's GitHub for the TCE example:

https://github.com/USEPA/Water_Treatment_Models/tree/master/PSDM (J. Burkhardt, 2020).

7.1 Extending the USEPA fouling approach

In the PSDM model of USEPA, equations (27) and (28) were not included. Contrarily, they were calculated separately and the values were inserted for each group in the script. Since the group of PFAS consists of many examples, that is a time-consuming effort. The nine groups, together with some PFAS example compounds, are shown in the USEPA code in **Figure 32**.

```
'chemical': {'halogenated alkenes': [1.0, 0.0], #default
              'trihalo-methanes': [1.0, 0.0],
              'aromatics': [0.9, 0.1],
              'nitro compounds': [0.75, 0.25],
              'chlorinated hydrocarbon': [0.59, 0.41],
              'phenols': [0.65, 0.35],
              'PNAs': [0.32, 0.68],
              'pesticides': [0., 0.05],
              'PFAS': {'PFBA': [0.82, 0.12],
                        'PFPeA': [0.67, 0.19],
                        'PFHxA': [0.55, 0.28],
                        'PFHpA': [0.44, 0.36],
                        'PFOA': [0.34, 0.44],
                        ...
...
```

Figure 32 Groups and subgroups of CECs with compound-specific parameters a and b
(J. Burkhardt, 2020). Yellow = for the compound PFHpA

The 'compound properties' sheet in *Example_PFHpA.xlsx* was extended with compound-specific fouling properties. This way, the QSPR relationships, equations (27) and (28), could be calculated. The Excel data was processed through the *process_input_data* function and the fouling parameters were introduced to the model. QSPR relationships for calculation of b1 and b2 were then inserted. All numbers in **Figure 32** were replaced by 'b1' and 'b2', except for 'halogenated alkenes'. The reason is that 'halogenated alkenes' is the default and used for organic-free waters. This way, if *water_type* is 'organic-free', then b1 and b2 are 1.0 and 0.0 respectively. *k_mult_pd* is then equal to 1, see **Figure 30(no fouling)**, so there is no Freundlich K reduction in case of organic-free background water.

The Python script for this small extension can be seen in **Figure 33**.

```
comp_data = process_input_data('Example_PFHpA_1.xlsx', sheet_name='Properties')

logKOW = comp_data.loc['logKOW']
κ2 = comp_data.loc['κ2']
Nam = comp_data.loc['Nam']
alpha = comp_data.loc['α']
Dz_hybrid = comp_data.loc['Dz(hybrid)']

b1 = -0.0624 * logKOW - 1.15 * np.log10(κ2) - 0.166 * Nam + 1.37
b2 = 0.0441 * alpha + 0.406 * Dz_hybrid - 0.25
```

Figure 33 Python code for processing compound fouling properties and calculating QSPRs

The fouling properties were found in the supplemental information of the PFAS article (J. B. Burkhardt et al., 2022). Regarding the PFAS compound PFHpA that was used as example in the thesis, calculated parameters b1 and b2 were returned as 0.43565 and 0.360309 respectively, which were close to the previously inserted constants (0.44 and 0.36) from **Figure 32(yellow)**. As the compound-specific fouling parameters remained almost the same, the BTC of PFHpA was also identical.

The compound-specific fouling parameters b1 ($= a$) and b2 ($= b$) were thus successfully and automatically calculated by adding QSPR equations based upon the extra input, instead of manually calculating and inserting them. By the extension, fouling is represented more theoretically, but also more input parameters regarding the compound are required.

7.2 Alternative fouling approach

The fouling approach applied in the PSDM by USEPA model was based upon the reduction of the Freundlich capacity parameter K. This is a good approach, as it is based on experimental equations, but also needs time and effort. The parameters used in the fouling equations have some uncertainty and are only available for certain compounds (groups) as it is time-consuming to determine them for all OMPs.

An alternative fouling approach in this thesis was adopted by reducing the carbon bed weight instead of the Freundlich parameter. In fact, NOM preloading reduces the amount of carbon available for OMPs to adsorb onto. It is thus a more simple idea to reduce the carbon weight by adjusting one parameter. Equation (29) was added to *psdm.py* in the initialization function of the *PSDM* class, so an additional parameter *Reduced bed weight* could be calculated.

$$\text{Reduced bed weight} = \text{original bed weight} * (1 - \left(\frac{\alpha}{100}\right)) \quad (29)$$

```
chem_type1 = 'PFAS'
water_type1 = 'Rhine'

chem_type2 = 'Fouling alternative (15%)'
water_type2 = 'Fouling alternative (15%)'
```

Figure 34 Input required for original and alternative fouling calculation

Figure 34 shows example input data in the *Notebook* for BTC prediction with fouling calculation. The number, e.g. 15, was extracted from the string and defined as α in the equation above. The *run_psdm_kfit* function was executed for different *columns*: a column considering no fouling, a column using the original fouling approach and a column using the alternative fouling approach. For all of them, the example of PFHpA from the pilot PFAS study (J. B. Burkhardt et al., 2022) was used. Further, lines were added to the notebook to automatically display a graph showing the BTC and a graph showing the Freundlich K parameter as function of time for each of the columns (**Figure 35**).

It can be seen from **Figure 35(a)** that the alternative fouling method, by carbon weight reduction, indeed moved the BTC towards the left. Thus, breakthrough occurred earlier as less carbon was available due to NOM preloading. However, 15% weight reduction seemed to be insufficient to fit the '*fouling (Rhine)*' curve, which perfectly fitted experimental data (**Figure 26**).

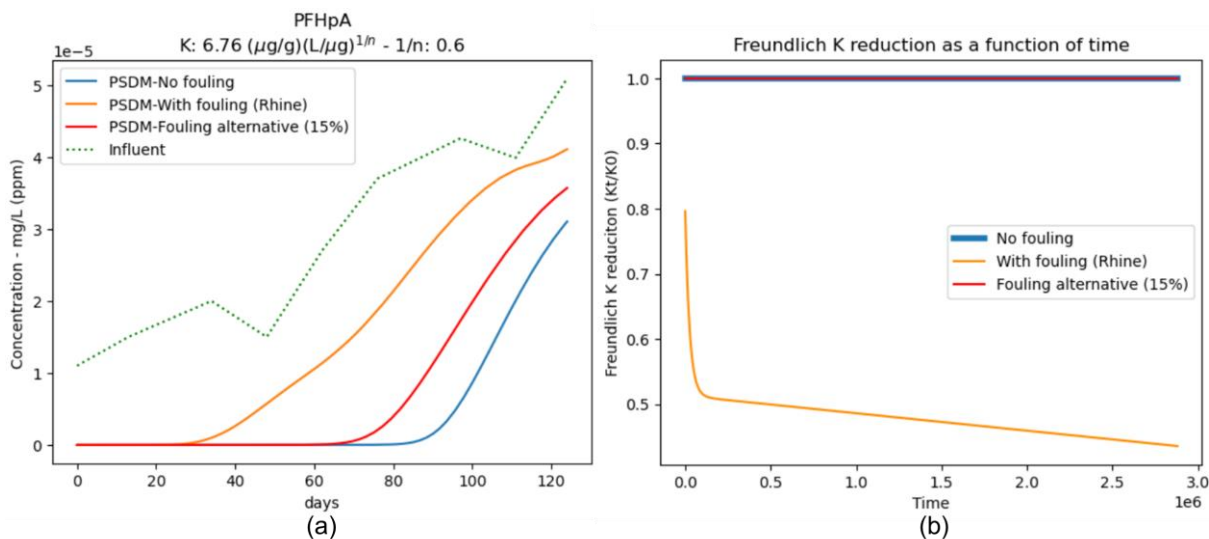


Figure 35 Comparison of original fouling (K reduction), alternative fouling (15% carbon weight reduction) and no fouling for fixed-bed adsorption of PFHpA: (a) breakthrough curve model prediction, (b) Freundlich K reduction

Figure 35(b) clearly confirms that there was no Freundlich K reduction for the *No fouling* or *Fouling alternative* curves. This to be sure that the alternative fouling method was purely based on carbon mass reduction. As this reduction was not sufficient, parameter α was calibrated onto experimental effluent data, which was earlier well-fitted by the '*fouling (Rhine)*' curve. The result is shown in **Figure 36**.

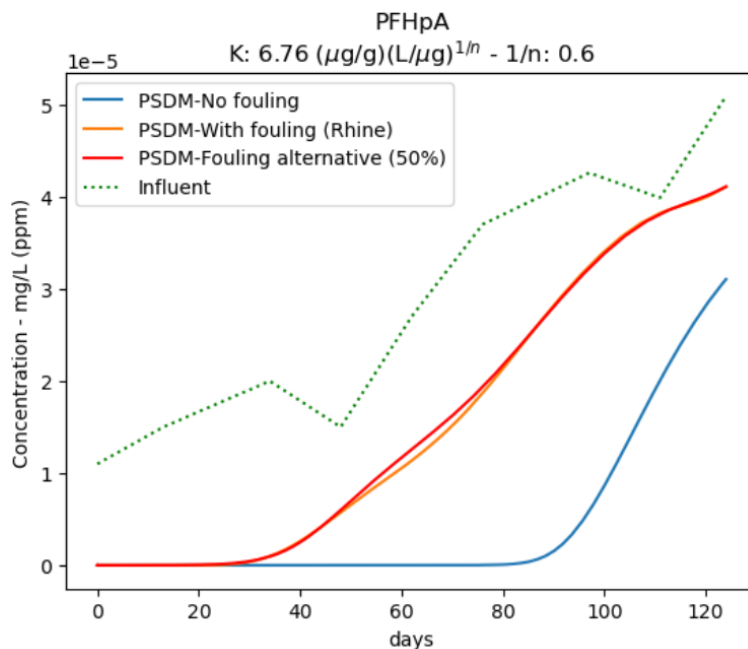


Figure 36 BTC model predictions for various fouling approaches; No fouling, K-reduction (t) and carbon weight reduction (50%)

It can be seen that reducing the amount of carbon with 50% resulted in a good fit. This leads to the conclusion that the impact of NOM on PFHpA adsorption from raw river water (J. B. Burkhardt et al., 2022) was high and approximately halved the amount of carbon available for adsorption. Advantages of the alternative method are that less parameters are needed and it is a simple, straightforward method. Disadvantages are that this approach is less theoretically grounded and capacity reduction by NOM is hard to estimate in terms of weight.

It also must be noted that the alternative fouling approach presented here was not time-dependent. The carbon bed weight initially is set to a lower value and keeps constant during the simulation, no matter how long NOM has been building up. However, the original approach, where Freundlich K was reduced, was not very time-dependent neither. This can be seen in **Figure 35(b)**; the curve is steep in the beginning, but quickly becomes linear and less critical.

7.3 Uncertainty analysis of Freundlich parameters

In this paragraph, it is explained how the PSDM model by USEPA was extended with an automatically returned visualization of the uncertainty of Freundlich parameters K and 1/n.

Data of compound PFHpA was again used as input for the model, the influent concentration was assumed constant for simplification. The amount (%) of uncertainty for parameters K and 1/n were included under *percent_K* and *percent_xn*, respectively. Copies were made of the isotherm data object '*k_data*' and the deviated isotherm parameters were stored there. These copies were assigned to different columns. The *run_psdm_kfit* function was executed for these columns, each having its own isotherm data. First the original BTC was plotted, then the BTCs with deviated isotherm parameters were added to the same graph. Uncertainty analysis was also done for the example compound TCE. The BTCs, with deviation of isotherm parameters, are illustrated for the compounds TCE and PFHpA in **Figure 37** and **Figure 38**, respectively. The amount (%) of uncertainty for parameters K and 1/n can be modified, causing the graph to adjust automatically.

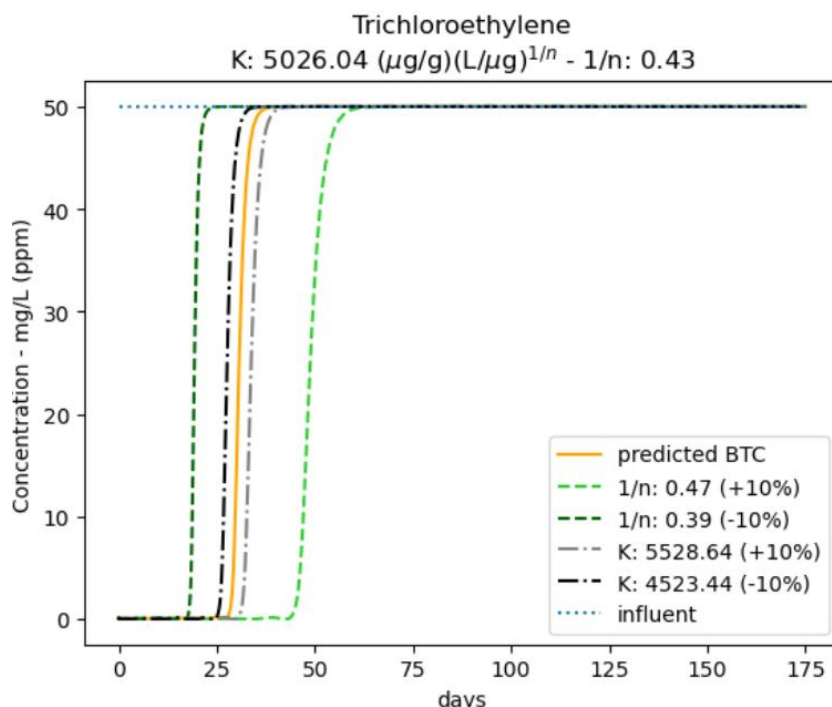


Figure 37 BTC prediction and uncertainty analysis with isotherm parameter uncertainty of 10%. Compound = TCE

Uncertainty of the isotherm parameters seems to play a significant role in prediction of bed replacement intervals. Only 10% uncertainty for the Freundlich 1/n parameter can result in more than 40% difference in breakthrough time. Considering the Freundlich isotherm relationship (equation (1)), it seems logical that higher values for isotherm parameters result in higher time before regeneration is needed. Namely, equilibrium adsorption capacity increases along with the equilibrium parameters.

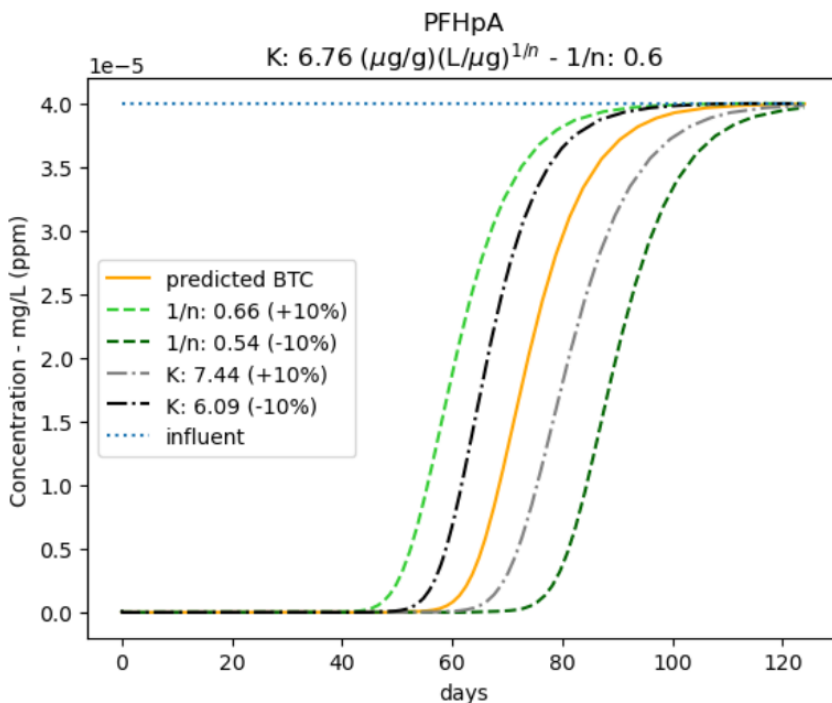


Figure 38 BTC prediction and uncertainty analysis with isotherm parameter uncertainty of 10%. Compound = PFHpA

For the compound PFHpA however (Figure 38), a strange behaviour for the parameter $1/n$ can be observed. Increasing the parameter $1/n$ does not lead to an increased adsorption capacity and thus increased breakthrough time. Instead, the opposite occurs. This phenomenon was further investigated by plotting the Freundlich isotherm equations for both compounds, including uncertainties. The script was also written so the isotherms were displayed automatically according to the amount of uncertainty.

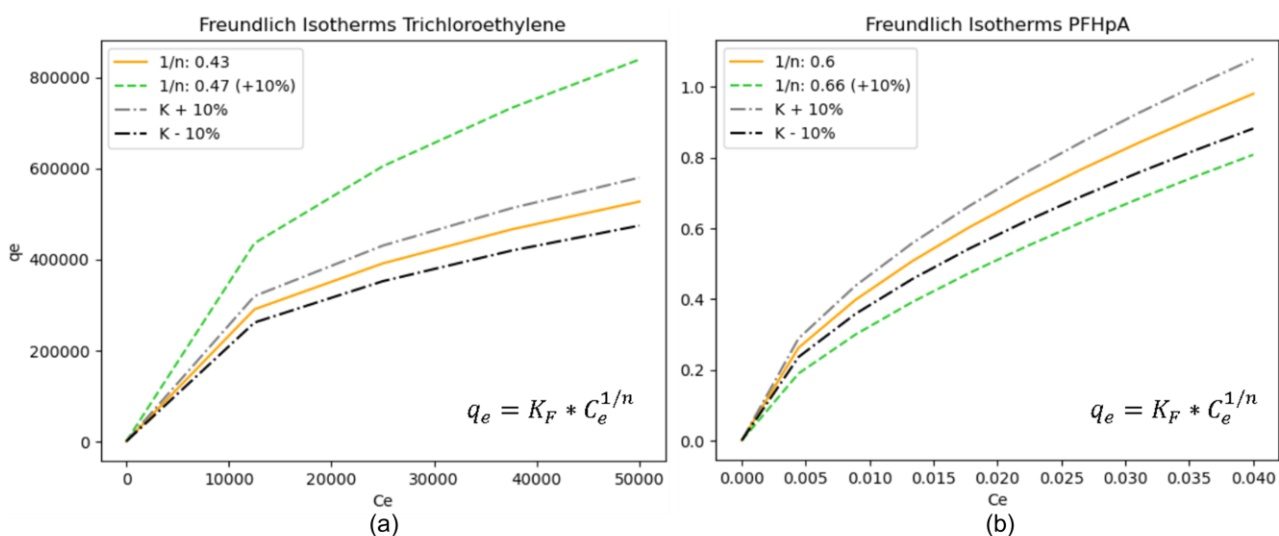


Figure 39 Freundlich isotherm equations with parameter uncertainty for compounds (a) TCE & (b) PFHpA

Figure 39 again represents the equation of the Freundlich isotherm and so one could expect that equilibrium adsorption capacity q_e would increase with increasing equilibrium parameters. This however was not always the case. The difference could be explained by the equilibrium concentration C_e . Concentration is > 1 in Figure 39(a) and < 1 in Figure 39(b). Because C_e is smaller than 1, increasing the exponent means decreasing the whole factor. This is why changing $1/n$ had an opposite effect.

8 THE PSDM MODEL FOR FULL-SCALE APPLICATION

8.1 The Interreg project

An example of a full-scale set-up for the removal of micropollutants in municipal wastewater is shown in **Figure 2**. After conventional treatment, some of the wastewater will be further filtered, followed by the advanced treatment processes. The advanced treatment here is a combination of ozonation and adsorption by granular activated carbon (GAC) in fixed-bed reactors. Ozonation is an oxidation process that will be beneficial for actually degrade part of the micropollutants, to avoid them only being relocated. On the other hand, ozonation without GAC would be too energy-intensive and causes problems with by-products (Aquafin, 2023; Guillossou et al., 2020).

- ***Which contaminants are my focus for conducting models? Is there a representative compound that can tell about all OMPs?***

Uitgangspunt in dit STOWA rapport is dat het te bereiken zuiveringsrendement een keuze is van de waterschappen, waarbij aangesloten kan worden op de door het ministerie van IenW vastgestelde bijdrageregeling 'Zuivering medicijnresten'. Voor de bijdrageregeling 'Zuivering medicijnresten' van het ministerie IenW gelden de volgende minimum eisen

- Een zuiveringsrendement moet worden gerealiseerd van 70%² verwijdering van 7 (van de 11) Nederlandse gidsstoffen: benzotriazool, clarithromycine, carbamazepine, diclofenac, metropolol, hydrochlorothiazide, mengsel van 4 en 5-methylbenzotriazool, propanolol, sotalol, sulfamethoxazol, trimethoprim. Dit rendement wordt berekend als gemiddelde waarde van de zuiveringsrendementen van de afzonderlijke 7 gidsstoffen in elk debiet- of tijdsproportioneel genomen watermonster op basis van het gemeten concentratieverschil van de betreffende gidsstof in ruw rioolwater/afloop voorbeziinthank en het effluent van
-
-

Simon: in the Netherlands there is a new legislation that it cannot be above 1 µg/L which is really low and challenging for standalone ozonation. That makes the combination with GAC even more interesting.

CONCLUSION

REFERENCE LIST

- Ahmadi, N., Abbasi, M., Torabian, A., van Loosdrecht, M. C. M., & Ducoste, J. (2023). Biotransformation of micropollutants in moving bed biofilm reactors under heterotrophic and autotrophic conditions. *Journal of Hazardous Materials*, 460, 132232. <https://doi.org/10.1016/j.jhazmat.2023.132232>
- Albuquerque, B., Heleno, S., Oliveira, M., Barros, L., & Ferreira, I. (2020). Phenolic compounds: Current industrial applications, limitations and future challenges. *Food & Function*. <https://doi.org/10.1039/D0FO02324H>
- Aliakbarian, B., Casazza, A., & Perego, P. (2015). Kinetic and Isotherm Modelling of the Adsorption of Phenolic Compounds from Olive Mill Wastewater onto Activated Carbon. *Food Technology and Biotechnology*, 53, 207–214.
- Aquafin. (2023). *Full-scale set-up for removal micropollutants*. <https://www.aquafin.be/en/full-scale-set-up-for-removal-micropollutants>
- Arvaniti, O. S., Dasenaki, M. E., Asimakopoulos, A. G., Maragou, N. C., Samaras, V. G., Antoniou, K., Gatidou, G., Mamaïs, D., Noutsopoulos, C., Frontistis, Z., Thomaidis, N. S., & Stasinakis, A. S. (2022). Effectiveness of tertiary treatment processes in removing different classes of emerging contaminants from domestic wastewater. *Frontiers of Environmental Science & Engineering*, 16(11), 148. <https://doi.org/10.1007/s11783-022-1583-y>
- Brandt, M. J., Johnson, K. M., Elphinston, A. J., & Ratnayaka, D. D. (2017). Chapter 10—Specialized and Advanced Water Treatment Processes. In M. J. Brandt, K. M. Johnson, A. J. Elphinston, & D. D. Ratnayaka (Eds.), *Twort's Water Supply (Seventh Edition)* (pp. 407–473). Butterworth-Heinemann. <https://doi.org/10.1016/B978-0-08-100025-0.00010-7>
- Burkhardt, J. (2020). *Water_Treatment_Models/PSDM at master · USEPA/Water_Treatment_Models · GitHub*. https://github.com/USEPA/Water_Treatment_Models/tree/master/PSDM
- Burkhardt, J. B., Burns, N., Mobley, D., Pressman, J. G., Magnuson, M. L., & Speth, T. F. (2022). Modeling PFAS Removal Using Granular Activated Carbon for Full-Scale System Design—

Supplemental information. *Journal of Environmental Engineering*, 148(3), 04021086.

[https://doi.org/10.1061/\(ASCE\)EE.1943-7870.0001964](https://doi.org/10.1061/(ASCE)EE.1943-7870.0001964)

Burkhardt, J., Burns, N., Mobley, D., Pressman, J. G., Magnuson, M. L., & Speth, T. F. (2022).

Modeling PFAS Removal Using Granular Activated Carbon for Full-Scale System Design.

Journal of Environmental Engineering, 148(3), 04021086.

[https://doi.org/10.1061/\(ASCE\)EE.1943-7870.0001964](https://doi.org/10.1061/(ASCE)EE.1943-7870.0001964)

Cantoni, B., Ianes, J., Bertolo, B., Ziccardi, S., Maffini, F., & Antonelli, M. (2024). Adsorption on activated carbon combined with ozonation for the removal of contaminants of emerging concern in drinking water. *Journal of Environmental Management*, 350, 119537.

<https://doi.org/10.1016/j.jenvman.2023.119537>

Das, S., Ray, N. M., Wan, J., Khan, A., Chakraborty, T., & Ray, M. B. (2017). Micropollutants in Wastewater: Fate and Removal Processes. In R. Farooq & Z. Ahmad (Eds.), *Physico-Chemical Wastewater Treatment and Resource Recovery*. InTech.

<https://doi.org/10.5772/65644>

Edefell, E., Falås, P., Torresi, E., Hagman, M., Cimbritz, M., Bester, K., & Christensson, M. (2021). Promoting the degradation of organic micropollutants in tertiary moving bed biofilm reactors by controlling growth and redox conditions. *Journal of Hazardous Materials*, 414, 125535.

<https://doi.org/10.1016/j.jhazmat.2021.125535>

European Investment Bank, & Bofill, J. (2023). *Microplastics and Micropollutants in Water: Contaminants of emerging concern*.

Guerra, P., Kim, M., Kinsman, L., Ng, T., Alaee, M., & Smyth, S. A. (2014). Parameters affecting the formation of perfluoroalkyl acids during wastewater treatment. *Journal of Hazardous Materials*, 272, 148–154. <https://doi.org/10.1016/j.jhazmat.2014.03.016>

Guillossou, R., Le Roux, J., Brosillon, S., Mailler, R., Vulliet, E., Morlay, C., Nauleau, F., Rocher, V., & Gaspéri, J. (2020). Benefits of ozonation before activated carbon adsorption for the removal of organic micropollutants from wastewater effluents. *Chemosphere*, 245, 125530.

<https://doi.org/10.1016/j.chemosphere.2019.125530>

Gutiérrez, M., Grillini, V., Mutavdžić Pavlović, D., & Verlicchi, P. (2021). Activated carbon coupled with advanced biological wastewater treatment: A review of the enhancement in micropollutant removal. *Science of The Total Environment*, 790, 148050.
<https://doi.org/10.1016/j.scitotenv.2021.148050>

Hokanson, D. R., Hand, D. W., Crittenden, J. C., Rogers, T. N., & Oman, E. J. (1999, July 23). *Michigan Technological University (MTU) Researchers Develop New Software To Help Clean Up Contamination Sites*. ScienceDaily.

<https://www.sciencedaily.com/releases/1999/07/990723083614.htm>

Inglezakis, V. J., Fyrillas, M. M., & Park, J. (2019). Variable diffusivity homogeneous surface diffusion model and analysis of merits and fallacies of simplified adsorption kinetics equations. *Journal of Hazardous Materials*, 367, 224–245. <https://doi.org/10.1016/j.jhazmat.2018.12.023>

Issabayeva, G., Hang, S., Wong, M., & Aroua, M. (2017). A review on the adsorption of phenols from wastewater onto diverse groups of adsorbents. *Reviews in Chemical Engineering*, 34.
<https://doi.org/10.1515/revce-2017-0007>

Jarvie, M. E., Hand, D. W., Bhuvendralingam, S., Crittenden, J. C., & Hokanson, D. R. (2005). Simulating the performance of fixed-bed granular activated carbon adsorbers: Removal of synthetic organic chemicals in the presence of background organic matter. *Water Research*, 39(11), 2407–2421. <https://doi.org/10.1016/j.watres.2005.04.023>

Khanzada, N. K., Farid, M. U., Kharraz, J. A., Choi, J., Tang, C. Y., Nghiem, L. D., Jang, A., & An, A. K. (2020). Removal of organic micropollutants using advanced membrane-based water and wastewater treatment: A review. *Journal of Membrane Science*, 598, 117672.
<https://doi.org/10.1016/j.memsci.2019.117672>

Kim, S.-K., Im, J.-K., Kang, Y.-M., Jung, S.-Y., Kho, Y. L., & Zoh, K.-D. (2012). Wastewater treatment plants (WWTPs)-derived national discharge loads of perfluorinated compounds (PFCs). *Journal of Hazardous Materials*, 201–202, 82–91.
<https://doi.org/10.1016/j.jhazmat.2011.11.036>

Krzeminski, P., Tomei, M. C., Karaolia, P., Langenhoff, A., Almeida, C. M. R., Felis, E., Gritten, F., Andersen, H. R., Fernandes, T., Manaia, C. M., Rizzo, L., & Fatta-Kassinos, D. (2019).

- Performance of secondary wastewater treatment methods for the removal of contaminants of emerging concern implicated in crop uptake and antibiotic resistance spread: A review. *Science of The Total Environment*, 648, 1052–1081.
<https://doi.org/10.1016/j.scitotenv.2018.08.130>
- Kumari, P., & Kumar, A. (2023). ADVANCED OXIDATION PROCESS: A remediation technique for organic and non-biodegradable pollutant. *Results in Surfaces and Interfaces*, 11, 100122.
<https://doi.org/10.1016/j.rsurfi.2023.100122>
- Ma, Y., Zhang, X., & Wen, J. (2021). Study on the Harm of Waste Activated Carbon and Novel Regeneration Technology of it. *IOP Conference Series: Earth and Environmental Science*, 769(2). <https://doi.org/10.1088/1755-1315/769/2/022047>
- Magnuson, M. L., & Speth, T. F. (2005). Quantitative Structure–Property Relationships for Enhancing Predictions of Synthetic Organic Chemical Removal from Drinking Water by Granular Activated Carbon. *Environmental Science & Technology*, 39(19), 7706–7711.
<https://doi.org/10.1021/es0508018>
- Mohammadi, F., Bina, B., Rahimi, S., & Janati, M. (2022). Modelling of micropollutant fate in hybrid growth systems: Model concepts, Peterson matrix, and application to a lab-scale pilot plant. *Environmental Science and Pollution Research*, 29. <https://doi.org/10.1007/s11356-022-20668-2>
- Mudhoo, A., Otero, M., & Chu, K. H. (2024). Insights into adsorbent tortuosity across aqueous adsorption systems. *Particuology*, 88, 71–88. <https://doi.org/10.1016/j.partic.2023.08.022>
- Ngeno, E. C., Mbuci, K. E., Necibi, M. C., Shikuku, V. O., Olisah, C., Ongulu, R., Matovu, H., Ssebugere, P., Abushaban, A., & Sillanpää, M. (2022). Sustainable re-utilization of waste materials as adsorbents for water and wastewater treatment in Africa: Recent studies, research gaps, and way forward for emerging economies. *Environmental Advances*, 9, 100282. <https://doi.org/10.1016/j.envadv.2022.100282>
- Patel, H. (2019). Fixed-bed column adsorption study: A comprehensive review. *Applied Water Science*, 9(3), 45. <https://doi.org/10.1007/s13201-019-0927-7>

Patel, H. (2022). Comparison of batch and fixed bed column adsorption: A critical review. *International Journal of Environmental Science and Technology*, 19(10), 10409–10426.

<https://doi.org/10.1007/s13762-021-03492-y>

Persson, L., Carney Almroth, B. M., Collins, C. D., Cornell, S., De Wit, C. A., Diamond, M. L., Fantke, P., Hassellöv, M., MacLeod, M., Ryberg, M. W., Søgaard Jørgensen, P., Villarrubia-Gómez, P., Wang, Z., & Hauschild, M. Z. (2022). Outside the Safe Operating Space of the Planetary Boundary for Novel Entities. *Environmental Science & Technology*, 56(3), 1510–1521.

<https://doi.org/10.1021/acs.est.1c04158>

Piazzoli, A., & Antonelli, M. (2018). Application of the Homogeneous Surface Diffusion Model for the prediction of the breakthrough in full-scale GAC filters fed on groundwater. *Process Safety and Environmental Protection*, 117, 286–295. <https://doi.org/10.1016/j.psep.2018.04.027>

Pocostales, J. P., Alvarez, P. M., & Beltrán, F. J. (2010). Kinetic modeling of powdered activated carbon ozonation of sulfamethoxazole in water. *Chemical Engineering Journal*, 164(1), 70–76. <https://doi.org/10.1016/j.cej.2010.08.025>

Rizzo, L., Malato, S., Antakyali, D., Beretsou, V. G., Đolić, M. B., Gernjak, W., Heath, E., Ivancev-Tumbas, I., Karaolia, P., Lado Ribeiro, A. R., Mascolo, G., Mc Ardell, C. S., Schaar, H., Silva, A. M. T., & Fatta-Kassinos, D. (2019). Consolidated vs new advanced treatment methods for the removal of contaminants of emerging concern from urban wastewater. *Science of The Total Environment*, 655, 986–1008. <https://doi.org/10.1016/j.scitotenv.2018.11.265>

Sabri, A., & Abbood, N. (2019). Adsorption Study of Nitrate Anions by Different Materials Using Fixed Bed Column. *Engineering and Technology Journal*, 37. <https://doi.org/10.30684/etj.37.1C.25>

Saidulu, D., Majumder, A., & Gupta, A. K. (2021). A systematic review of moving bed biofilm reactor, membrane bioreactor, and moving bed membrane bioreactor for wastewater treatment: Comparison of research trends, removal mechanisms, and performance. *Journal of Environmental Chemical Engineering*, 9(5), 106112.

<https://doi.org/10.1016/j.jece.2021.106112>

- Saleh, T. A. (2022). Chapter 4—Isotherm models of adsorption processes on adsorbents and nanoadsorbents. In T. A. Saleh (Ed.), *Interface Science and Technology* (Vol. 34, pp. 99–126). Elsevier. <https://doi.org/10.1016/B978-0-12-849876-7.00009-9>
- Şerban, G., Iancu, V.-I., Dinu, C., Tenea, A., Vasilache, N., Cristea, I., Niculescu, M., Ionescu, I., & Chiriac, F. L. (2023). Removal Efficiency and Adsorption Kinetics of Methyl Orange from Wastewater by Commercial Activated Carbon. *Sustainability*, 15, 1–17. <https://doi.org/10.3390/su151712939>
- Sharifian, S., & Asasian-Kolur, N. (2022). Polyethylene terephthalate (PET) waste to carbon materials: Theory, methods and applications. *Journal of Analytical and Applied Pyrolysis*, 163, 105496. <https://doi.org/10.1016/j.jaap.2022.105496>
- Sharma, S., Balestra, S. R. G., Baur, R., Agarwal, U., Zuidema, E., Rigutto, M. S., Calero, S., Vlugt, T. J. H., & Dubbeldam, D. (2023). RUPTURA: Simulation code for breakthrough, ideal adsorption solution theory computations, and fitting of isotherm models. *Molecular Simulation*, 49(9), 893–953. <https://doi.org/10.1080/08927022.2023.2202757>
- Sharma, V., & Feng, M. (2017). Water depollution using metal-organic frameworks-catalyzed advanced oxidation processes: A review. *Journal of Hazardous Materials*, 372. <https://doi.org/10.1016/j.jhazmat.2017.09.043>
- Silva, L. M. S., Muñoz-Peña, M. J., Domínguez-Vargas, J. R., González, T., & Cuerda-Correa, E. M. (2021). Kinetic and equilibrium adsorption parameters estimation based on a heterogeneous intraparticle diffusion model. *Surfaces and Interfaces*, 22, 100791. <https://doi.org/10.1016/j.surfin.2020.100791>
- Sookkumnerd, T. (2019). Numerical Modeling of Industrial-Scale Pulsed Bed Adsorber for Colorant Removal in Sugar Refining. *IOP Conference Series: Materials Science and Engineering*, 559, 012019. <https://doi.org/10.1088/1757-899X/559/1/012019>
- Spindola Vilela, C. L., Damasceno, T. L., Thomas, T., & Peixoto, R. S. (2022). Global qualitative and quantitative distribution of micropollutants in the deep sea. *Environmental Pollution*, 307, 119414. <https://doi.org/10.1016/j.envpol.2022.119414>

The BAC Process for Water Purification. (2000, December). Wastewater Digest.

<https://www.wwdmag.com/wastewater-treatment/article/10917010/the-biological-activated-carbon-process-for-water-purification>

Topolovec, B., Škoro, N., Puač, N., & Petrović, M. (2022). Pathways of organic micropollutants degradation in atmospheric pressure plasma processing – A review. *Chemosphere*, 294, 133606. <https://doi.org/10.1016/j.chemosphere.2022.133606>

Trojanowicz, M. (2020). Removal of persistent organic pollutants (POPs) from waters and wastewaters by the use of ionizing radiation. *Science of The Total Environment*, 718, 134425. <https://doi.org/10.1016/j.scitotenv.2019.134425>

Vanoppen, M. (2023). 6 Activated Carbon Filtration. In *Environmental Technology: Water*. UGent-BW.

Wang, J., & Guo, X. (2020). Adsorption isotherm models: Classification, physical meaning, application and solving method. *Chemosphere*, 258, 127279. <https://doi.org/10.1016/j.chemosphere.2020.127279>

Wang, J., & Guo, X. (2023). Adsorption kinetics and isotherm models of heavy metals by various adsorbents: An overview. *Critical Reviews in Environmental Science and Technology*, 53(21), 1837–1865. <https://doi.org/10.1080/10643389.2023.2221157>

Webb, P. A. (2001). *Volume and Density Determinations for Particle Technologists*.

Westerhoff, P., Yoon, Y., Snyder, S., & Wert, E. (2005). Fate of Endocrine-Disruptor, Pharmaceutical, and Personal Care Product Chemicals during Simulated Drinking Water Treatment Processes. *Environmental Science & Technology*, 39(17), 6649–6663. <https://doi.org/10.1021/es0484799>

Worch, E. (2008). Fixed-bed adsorption in drinking water treatment: A critical review on models and parameter estimation. *Journal of Water Supply Research and Technology-Aqua - J WATER SUPPLY RES TECHNOL-AQ*, 57. <https://doi.org/10.2166/aqua.2008.100>

Xiaojian, Z., Zhansheng, W., & Xiasheng, G. (1991). Simple combination of biodegradation and carbon adsorption—The mechanism of the biological activated carbon process. *Water Research*, 25(2), 165–172. [https://doi.org/10.1016/0043-1354\(91\)90025-L](https://doi.org/10.1016/0043-1354(91)90025-L)

Xu, Z., Cai, J., & Pan, B. (2013). Mathematically modeling fixed-bed adsorption in aqueous systems.

Journal of Zhejiang University SCIENCE A, 14(3), 155–176.

<https://doi.org/10.1631/jzus.A1300029>

Yao, C., & Zhu, C. (2021). A new multi-mechanism adsorption kinetic model and its relation to mass transfer coefficients. *Surfaces and Interfaces*, 26, 101422.

<https://doi.org/10.1016/j.surfin.2021.101422>

Yin, R., & Shang, C. (2020). Removal of micropollutants in drinking water using UV-LED/chlorine advanced oxidation process followed by activated carbon adsorption. *Water Research*, 185, 116297. <https://doi.org/10.1016/j.watres.2020.116297>

Zahmatkesh, S., Amesho, K. T. T., & Sillanpää, M. (2022). A critical review on diverse technologies for advanced wastewater treatment during SARS-CoV-2 pandemic: What do we know? *Journal of Hazardous Materials Advances*, 7, 100121.

<https://doi.org/10.1016/j.hazadv.2022.100121>

Zahmatkesh, S., Bokhari, A., Karimian, M., Zahra, M. M. A., Sillanpää, M., Panchal, H., Alrubaie, A. J., & Rezakhani, Y. (2022). A comprehensive review of various approaches for treatment of tertiary wastewater with emerging contaminants: What do we know? *Environmental Monitoring and Assessment*, 194(12), 884. <https://doi.org/10.1007/s10661-022-10503-z>

Zhou, L., Qu, Z. G., Ding, T., & Miao, J. Y. (2016). Lattice Boltzmann simulation of the gas-solid adsorption process in reconstructed random porous media. *Physical Review E*, 93(4), 043101. <https://doi.org/10.1103/PhysRevE.93.043101>

APPENDICES

1. < datum - {dd-mm-jj} > : < titel >
- 2.